



---

**Constrained Optimization Paradigms for Adaptive, Cognitive Radar**

**Vishal Monga**  
**PENNSYLVANIA STATE UNIVERSITY**

---

**11/28/2018**  
**Final Report**

DISTRIBUTION A: Distribution approved for public release.

Air Force Research Laboratory  
AF Office Of Scientific Research (AFOSR)/ RTB1  
Arlington, Virginia 22203  
Air Force Materiel Command

**REPORT DOCUMENTATION PAGE**

Form Approved  
OMB No. 0704-0188

The public reporting burden for this collection of information is estimated to average 1 hour per response, including the time for reviewing instructions, searching existing data sources, gathering and maintaining the data needed, and completing and reviewing the collection of information. Send comments regarding this burden estimate or any other aspect of this collection of information, including suggestions for reducing the burden, to the Department of Defense, Executive Service Directorate (0704-0188). Respondents should be aware that notwithstanding any other provision of law, no person shall be subject to any penalty for failing to comply with a collection of information if it does not display a currently valid OMB control number.

**PLEASE DO NOT RETURN YOUR FORM TO THE ABOVE ORGANIZATION.**

<b>1. REPORT DATE (DD-MM-YYYY)</b> 14-09-2018		<b>2. REPORT TYPE</b> Final Report		<b>3. DATES COVERED (From - To)</b> 15 September 2015 - 14 September 2018	
<b>4. TITLE AND SUBTITLE</b> Constrained Optimization Paradigms for Adaptive, Cognitive Radar				<b>5a. CONTRACT NUMBER</b>	
				<b>5b. GRANT NUMBER</b> FA9550-15-1-0438	
				<b>5c. PROGRAM ELEMENT NUMBER</b>	
<b>6. AUTHOR(S)</b> Monga, Vishal				<b>5d. PROJECT NUMBER</b>	
				<b>5e. TASK NUMBER</b>	
				<b>5f. WORK UNIT NUMBER</b>	
<b>7. PERFORMING ORGANIZATION NAME(S) AND ADDRESS(ES)</b> The Pennsylvania State University, University Park, PA 16802				<b>8. PERFORMING ORGANIZATION REPORT NUMBER</b>	
<b>9. SPONSORING/MONITORING AGENCY NAME(S) AND ADDRESS(ES)</b> AFOSR/JA (703) 696-9705 875 North Randolph Street, Suite 325, Room 3112m Arlington, VA 22203				<b>10. SPONSOR/MONITOR'S ACRONYM(S)</b>	
				<b>11. SPONSOR/MONITOR'S REPORT NUMBER(S)</b>	
<b>12. DISTRIBUTION/AVAILABILITY STATEMENT</b> DISTRIBUTION A					
<b>13. SUPPLEMENTARY NOTES</b>					
<b>14. ABSTRACT</b> Multiple-Input Multiple-Output (MIMO) radar system allows each antenna element to transmit a different waveform. This waveform diversity can be exploited to enhance the beampattern design, in particular, effective management of radar radiation power in directions of interest. This work addresses the problem of designing a beampattern for MIMO radar, which in turn is determined by the transmit waveform. While unconstrained design is straightforward, a key open challenge is enforcing the constant modulus constraint on the radar waveform. It is well-known that the problem of minimizing deviation of the designed beampattern vs. an idealized one subject to the constant modulus constraint constitutes a hard non-convex problem. Existing methods that address constant modulus invariably lead to a stiff trade-off between analytical tractability (achieved by relaxations and approximations) and realistic design that exactly achieves constant modulus but is computationally burdensome. A new approach is proposed in this work, which involves solving a sequence of convex Equality Constrained Quadratic Programs, each of which has a closed form solution and such that constant modulus is achieved at convergence.					
<b>15. SUBJECT TERMS</b> MIMO radar, waveform design, constant modulus, similarity constraint, cognitive radar					
<b>16. SECURITY CLASSIFICATION OF:</b>			<b>17. LIMITATION OF ABSTRACT</b>	<b>18. NUMBER OF PAGES</b>	<b>19a. NAME OF RESPONSIBLE PERSON</b>
<b>a. REPORT</b>	<b>b. ABSTRACT</b>	<b>c. THIS PAGE</b>			<b>19b. TELEPHONE NUMBER (Include area code)</b>

Reset

## INSTRUCTIONS FOR COMPLETING SF 298

**1. REPORT DATE.** Full publication date, including day, month, if available. Must cite at least the year and be Year 2000 compliant, e.g. 30-06-1998; xx-06-1998; xx-xx-1998.

**2. REPORT TYPE.** State the type of report, such as final, technical, interim, memorandum, master's thesis, progress, quarterly, research, special, group study, etc.

**3. DATES COVERED.** Indicate the time during which the work was performed and the report was written, e.g., Jun 1997 - Jun 1998; 1-10 Jun 1996; May - Nov 1998; Nov 1998.

**4. TITLE.** Enter title and subtitle with volume number and part number, if applicable. On classified documents, enter the title classification in parentheses.

**5a. CONTRACT NUMBER.** Enter all contract numbers as they appear in the report, e.g. F33615-86-C-5169.

**5b. GRANT NUMBER.** Enter all grant numbers as they appear in the report, e.g. AFOSR-82-1234.

**5c. PROGRAM ELEMENT NUMBER.** Enter all program element numbers as they appear in the report, e.g. 61101A.

**5d. PROJECT NUMBER.** Enter all project numbers as they appear in the report, e.g. 1F665702D1257; ILIR.

**5e. TASK NUMBER.** Enter all task numbers as they appear in the report, e.g. 05; RF0330201; T4112.

**5f. WORK UNIT NUMBER.** Enter all work unit numbers as they appear in the report, e.g. 001; AFAPL30480105.

**6. AUTHOR(S).** Enter name(s) of person(s) responsible for writing the report, performing the research, or credited with the content of the report. The form of entry is the last name, first name, middle initial, and additional qualifiers separated by commas, e.g. Smith, Richard, J, Jr.

**7. PERFORMING ORGANIZATION NAME(S) AND ADDRESS(ES).** Self-explanatory.

**8. PERFORMING ORGANIZATION REPORT NUMBER.** Enter all unique alphanumeric report numbers assigned by the performing organization, e.g. BRL-1234; AFWL-TR-85-4017-Vol-21-PT-2.

**9. SPONSORING/MONITORING AGENCY NAME(S) AND ADDRESS(ES).** Enter the name and address of the organization(s) financially responsible for and monitoring the work.

**10. SPONSOR/MONITOR'S ACRONYM(S).** Enter, if available, e.g. BRL, ARDEC, NADC.

**11. SPONSOR/MONITOR'S REPORT NUMBER(S).** Enter report number as assigned by the sponsoring/monitoring agency, if available, e.g. BRL-TR-829; -215.

**12. DISTRIBUTION/AVAILABILITY STATEMENT.** Use agency-mandated availability statements to indicate the public availability or distribution limitations of the report. If additional limitations/ restrictions or special markings are indicated, follow agency authorization procedures, e.g. RD/FRD, PROPIN, ITAR, etc. Include copyright information.

**13. SUPPLEMENTARY NOTES.** Enter information not included elsewhere such as: prepared in cooperation with; translation of; report supersedes; old edition number, etc.

**14. ABSTRACT.** A brief (approximately 200 words) factual summary of the most significant information.

**15. SUBJECT TERMS.** Key words or phrases identifying major concepts in the report.

**16. SECURITY CLASSIFICATION.** Enter security classification in accordance with security classification regulations, e.g. U, C, S, etc. If this form contains classified information, stamp classification level on the top and bottom of this page.

**17. LIMITATION OF ABSTRACT.** This block must be completed to assign a distribution limitation to the abstract. Enter UU (Unclassified Unlimited) or SAR (Same as Report). An entry in this block is necessary if the abstract is to be limited.

## FINAL PROGRESS SUMMARY

- Contract/Grant Title: Constrained Optimization Paradigms for Adaptive, Cognitive Radar.
- Contract/Grant #: FA9550-15-1-0438
- Reporting Period: 15 September 2015 - 14 September 2018
- Project accomplishments (200 words max):

This work addresses the problem of designing a transmit waveform for multiple-input multiple-output (MIMO) radar under the important practical constraints of constant modulus, waveform similarity and the spectral interference constraints. Incorporating these constraints in an analytically tractable manner is a longstanding open challenge. This is due to the fact that the optimization problems that result either from signal to interference plus noise ratio (SINR) maximization or transmit beampattern design (minimizing deviation of the designed beampattern vs. an idealized one) subject to these constraints are in general hard non-convex problems. This project contributes a sequence of convex problems approach for solving the aforementioned hard non-convex problems. For SINR maximization, we developed the following approach:

  - Under constant modulus and similarity constraints: **Successive QCQP refinement (SQR) algorithm.**

For transmit beampattern design, we developed the following two approaches:

- Constant modulus constraint: **Successive closed form solutions (SCF) algorithm.**
  - Constant modulus and spectral interference constraints: **Beampattern optimization under interference and the constant modulus constraint (BIC) algorithm.**
- Archival publications (published) during reporting period:
    1. O. Aldayel, V. Monga and M. Rangaswamy, “SQR: Successive QCQP Refinement for MIMO Radar Waveform Design,” *IEEE Asilomar Conference on Signals, Systems and Computers*, pp. 85-89, November 2015, **Finalist for the Best Student Paper Award.**
    2. O. Aldayel, V. Monga and M. Rangaswamy, “Tractable MIMO Beampattern Design under Constant Modulus Waveform Constraint,” *IEEE Radar Conference*, May 2016
    3. O. Aldayel, V. Monga, and M. Rangaswamy, “Successive QCQP Refinement for MIMO Radar Waveform Design Under Practical Constraints,” *IEEE Transactions on Signal Processing*, vol. 64, no. 14, pp. 3760-3773, July 2016
    4. O. Aldayel, V. Monga, and M. Rangaswamy, “Tractable Transmit MIMO Beampattern Design Under a Constant Modulus Constraint,” *IEEE Transactions on Signal Processing*, vol. 65, no. 10, pp. 2588-2599, May 2017.
    5. B. Kang, O. Aldayel, V. Monga, and M. Rangaswamy, “Joint Design of Waveform and Receive Filter for MIMO Radar using Parametric Programming,” *IEEE Asilomar Conference on Signals, Systems and Computers*, November 2016.
    6. O. Aldayel, V. Monga, and M. Rangaswamy, “Adaptive Sequential Refinement for Ambiguity Function Shaping in Cognitive Radar,” *IEEE Asilomar Conference on Signals, Systems and Computers*, November 2017, **Finalist for the Best Student Paper Award.**
    7. B. Kang, O. Aldayel, V. Monga, and M. Rangaswamy, “Spatio-Spectral Radar Beampattern Design for Co-existence with Wireless Communication Systems,” accepted to *IEEE Transactions on Aerospace and Electronic Systems*, 2018.

- Changes in research objectives, if any: None
- Change in AFOSR program manager, if any: None
- Extensions granted or milestones slipped, if any: None
- Include any new discoveries, inventions, or patent disclosures during this reporting period (if none, report none): None

# Constrained Optimization Paradigms for Adaptive, Cognitive Radar

Vishal Monga

Department of Electrical Engineering  
The Pennsylvania State University,  
University Park, PA, USA

# Contents

<b>1</b>	<b>Summary of Accomplishments</b>	<b>3</b>
<b>2</b>	<b>Successive QCQP Refinement for MIMO Radar Waveform Design Under Practical Constraints</b>	<b>5</b>
2.1	Summary . . . . .	5
2.2	Introduction . . . . .	5
2.2.1	MIMO Signal Model . . . . .	5
2.2.2	Problem Formulation . . . . .	6
2.3	Methods, Assumptions, and Procedures . . . . .	6
2.3.1	Overview of Contribution . . . . .	6
2.3.2	Successive QCQP Refinement . . . . .	7
2.3.3	Joint Optimization of Waveform and Receive Filter . . . . .	10
2.4	Results and Discussions . . . . .	11
2.4.1	Experimental Setup and Methods Compared . . . . .	11
2.4.2	Experimental Evaluation . . . . .	11
2.5	Conclusions . . . . .	15
<b>3</b>	<b>Tractable Transmit MIMO Beampattern Design Under a Constant Modulus Constraint</b>	<b>16</b>
3.1	Summary . . . . .	16
3.2	Introduction . . . . .	17
3.2.1	System Model . . . . .	17
3.2.2	Problem Formulation . . . . .	18
3.3	Methods, Assumptions, and Procedures . . . . .	18
3.3.1	Overview of Contribution . . . . .	18
3.3.2	Sequence of Closed Forms Solutions . . . . .	19
3.4	Results and Discussions . . . . .	23
3.4.1	Narrowband null forming beampattern . . . . .	23
3.4.2	Wideband beampattern . . . . .	26
3.5	Conclusions . . . . .	33
<b>4</b>	<b>Spatio-Spectral Radar Beampattern Design for Co-existence with Wireless Communication Systems</b>	<b>34</b>
4.1	Summary . . . . .	34
4.1.1	Motivation and Challenges . . . . .	34
4.2	Introduction . . . . .	35
4.2.1	System Model . . . . .	35
4.2.2	Far-Field Beampattern . . . . .	35
4.2.3	Formulation of the Spectral Constraint . . . . .	36
4.2.4	Problem Formulation . . . . .	36
4.3	Methods, Assumptions, and Procedures . . . . .	37
4.3.1	Overview of Contribution . . . . .	37
4.4	Beampattern Design under Constant Modulus and Spectral Constraints . . . . .	38

4.4.1	Non-convex Optimization Problem . . . . .	38
4.4.2	Sequence of Closed Form Solutions . . . . .	39
4.4.3	Special Case: Nullforming Beampattern Design . . . . .	44
4.5	Results and Discussions . . . . .	45
4.5.1	Nullforming Beampattern Design . . . . .	46
4.5.2	Full Beampattern Design . . . . .	46
4.6	Conclusion . . . . .	47

# Chapter 1

## Summary of Accomplishments

Waveform design is one of the central aspects of radar systems. It can determine many of the radar properties. A well-designed waveform can improve the signal-to-interference-plus-noise ratio (SINR), enable suitable delay (range) resolution, and utilize the spectrum efficiently. Moreover, for multiple array radar system, waveform diversity can be employed to enhance the flexibility of the transmit beampattern design and enable efficient management of radar radiation power in directions of interest. While unconstrained waveform design is straightforward, a key open challenge is to enforce some of the significant practical constraints of constant modulus, waveform similarity and spectral interference constraints. Incorporating these constraints in an analytically tractable manner is a longstanding open challenge. This is due to the fact that the optimization problem subject to these constraints is a hard non-convex problem. Decades of the past work have shown a stiff trade-off between analytical tractability (achieved by relaxations to manageable constraints) and realistic design that exactly obeys these practical constraints but is computationally troublesome. In this work, we propose a new framework that breaks this classical trade-off.

In the first part, we address the problem of a joint transmit waveform and receive filter design for radar systems under the important practical constraints of constant modulus and waveform similarity. We develop a new analytical approach that involves solving a sequence of convex Quadratically Constrained Quadratic Programming (QCQP) problems, which we prove converges to a sub-optimal solution. Because an improvement in SINR results via solving each problem in the sequence, we call the method Successive QCQP Refinement (SQR). We evaluate SQR against other candidate techniques with respect to SINR performance, beampattern and pulse compression properties in a variety of scenarios. Results show that SQR outperforms state of the art methods that also employ constant modulus and/or similarity constraints while being computationally less burdensome.

In the second part, we address the problem of designing a beampattern for Multiple-Input-Multiple-Output (MIMO) radar, which in turn is determined by the transmit waveform. A new approach is proposed in our work, which involves solving the hard non-convex problem of beampattern design using a sequence of convex equality constrained Quadratic Programs (QP), each of which has a closed form solution. The converged solution achieves constant modulus and satisfies the KarushKuhnTucker (KKT) optimality conditions, which we prove formally is possible under realistic assumptions. We evaluate the proposed successive closed forms (SCF) algorithm against state-of-the-art MIMO beampattern design techniques and show that SCF breaks the trade-off between desirable performance and the associated computation cost.

In the third part, we address the problem of designing a beampattern for MIMO radar under a spectral interference constraint, which in turn is determined by the transmitted waveform, as well as the constant modulus constraint. One key challenge when jointly enforcing the spectral interference constraint and the constant modulus constraint is to ensure feasibility of the optimization problem. A new approach is proposed in our work, which also involves solving a sequence of constrained quadratic programs, each of which results in a closed form solution. We formally prove that feasible set of each QP problem in the proposed beampattern optimization under interference constraint and the constant modulus constraint (BIC) algorithm is always non-empty. We evaluate BIC algorithm against

the state-of-the-art MIMO beampattern design techniques under the constant modulus constraint and show that BIC achieves a higher performance while maintaining a low spectral interference level in the desired bands.

### Significant highlights related to project personnel

- B. Kang finished his PhD at Penn State and joined as a Radar Research Mathematician at the Wright State Research Institute (in Sep 2017) working closely with M. Rangaswamy and his group at the US Air Force Research Lab in Dayton, OH.
- Dr. B. Kang received the 2016 Robert T. Hill Memorial Outstanding Dissertation Award from the IEEE AESS for work supported by this project.
- O. Aldayel's work has had two best student paper finalists at IEEE Asilomar 2015 and 2017 respectively. Aldayel defended and started his academic position in Fall 2018.

## Chapter 2

# Successive QCQP Refinement for MIMO Radar Waveform Design Under Practical Constraints

### 2.1 Summary

The resolution and target detection performance of a radar are highly dependent on its signal waveform shape. A well designed (optimized) waveform can significantly improve the signal-to-interference-plus-noise ratio (SINR) [1, ?] and probability of detection [2, 3]. Other design criterion include desirable autocorrelation[4], suitable ambiguity function shaping [5, 6, 7], mutual information [8, 9, 10, 3] and beam pattern [11, 12, 13]. Further, with the advances in multiple-input multiple-output (MIMO) radar sensing, waveform design becomes more challenging since the design must allow for exploiting spatial diversity. Despite significant advances in radar waveform design, many practical challenges remain. One such challenge is the hardware requirement of a constant modulus waveform signal. Another challenge is to produce a design that does not compromise the autocorrelation properties by enforcing a strong similarity constraint. A vast majority of existing work however either ignores or relaxes [14] these constraints in favor of tractable analytical solutions. Meanwhile, this work achieves tractable waveform design for MIMO radar in the presence of constant modulus and similarity constraints. The central idea of the analytical contribution is to successively refine and achieve constant modulus at convergence, while solving a sequence of quadratically constrained quadratic programs, such that each optimization in the sequence satisfies a similarity constraint. This approach called SQR can achieve superior SINR and beam pattern with desirable suppression results against state of the art, remarkably at a lower computational cost. As an extension of the proposed SQR, we develop joint optimization of the waveform and receive filter using the parametric programming approach.

### 2.2 Introduction

#### 2.2.1 MIMO Signal Model

Consider a colocated narrow band MIMO radar system with  $N_T$  transmit antennas and  $N_R$  receive antennas. Each transmit element emits a different waveform  $x_m\{n\}$ ,  $m = 1, \dots, N_T$ ,  $n = 1, \dots, N$  where  $N$  is the number of samples. Let  $\mathbf{x}\{n\}$  be an  $N_T \times 1$  vector denoting the  $n$ -th sample of the  $N_T$  antennas. In addition, let  $\mathbf{x}$  be the concatenated and complete  $N_T N \times 1$  vector of the transmit waveform,  $\mathbf{x} = [\mathbf{x}^T\{1\}, \dots, \mathbf{x}^T\{N\}]^T$ . Then we have the following signal model[15]:

$$\mathbf{r} = \alpha_0 \mathbf{U}(\theta_0) \mathbf{x} + \sum_{k=1}^K \alpha_k \mathbf{U}(\theta_k) \mathbf{x} + \mathbf{n} \quad (2.1)$$

where  $\mathbf{r}$  is an  $N_R N \times 1$  receive waveform,  $\mathbf{n}$  is an  $N_R N \times 1$  circular complex Gaussian noise vector with zero mean and covariance matrix  $\sigma_n^2 \mathbf{I}$ ,  $\alpha_0$  and  $\alpha_k$  denote respectively to the complex amplitudes of the target and the  $k$ -th clutter source,  $\theta_0$  and  $\theta_k$  are the angle of the target and the angle of the  $k$ -th clutter source, respectively and  $\mathbf{U}(\theta)$  is the steering matrix of a uniform linear array (ULA) antenna with half-wavelength separation between the antennas given as:  $\mathbf{U}(\theta) = \mathbf{I}_N \otimes [\mathbf{a}_r(\theta)\mathbf{a}_t(\theta)^T]$  where  $\mathbf{I}_N$  is the  $N \times N$  identity matrix,  $\mathbf{a}_t$  and  $\mathbf{a}_r$  are the transmit and receive steering vector, respectively, as defined in [15].

The most common criterion in waveform design involves SINR maximization, which involves a joint optimization of the transmit waveform and the receive filter. In particular, the receive filter is assumed to be a linear finite impulse response (FIR) filter  $\mathbf{w} \in \mathbb{C}^{N_R N}$ . In this case, the output of filter  $r_f$  can be given by:

$$r_f = \mathbf{w}^H \mathbf{r} = \alpha_0 \mathbf{w}^H \mathbf{U}(\theta_0) \mathbf{x} + \sum_{k=1}^K \alpha_k \mathbf{w}^H \mathbf{U}(\theta_k) \mathbf{x} + \mathbf{w}^H \mathbf{n} \quad (2.2)$$

Therefore, the SINR can be expressed as:

$$SINR = \frac{\sigma |\mathbf{w}^H \mathbf{U}(\theta_0) \mathbf{x}|^2}{\mathbf{w}^H \boldsymbol{\Sigma}(\mathbf{x}) \mathbf{w} + \mathbf{w}^H \mathbf{w}} \quad (2.3)$$

where  $\sigma = E[|\alpha_0|^2]/\sigma_n^2$  and  $\boldsymbol{\Sigma}(\mathbf{x}) = \sum_{k=1}^K I_k \mathbf{U}(\theta_k) \mathbf{x} \mathbf{x}^H \mathbf{U}^H(\theta_k)$  where  $I_k = E[|\alpha_k|^2]/\sigma_n^2$ .

## 2.2.2 Problem Formulation

Our objective is to optimize the SINR in eq. (2.3) subject to the CMC and SC, i.e, solve the following optimization problem:

$$\begin{cases} \max_{\mathbf{w}, \mathbf{x}} & \frac{\sigma |\mathbf{w}^H \mathbf{U}(\theta_0) \mathbf{x}|^2}{\mathbf{w}^H \boldsymbol{\Sigma}(\mathbf{x}) \mathbf{w} + \mathbf{w}^H \mathbf{w}} \\ \text{s.t.} & \|\mathbf{x} - \mathbf{x}_0\|_\infty \leq \epsilon \\ & |\mathbf{x}(k)| = 1/\sqrt{N_T N} \end{cases} \quad (2.4)$$

where  $\mathbf{x}(k)$  is the  $k$ -th element of  $\mathbf{x}$ . It has been shown in [15] that the joint optimization problem of eq. (2.4) is equivalent to the following optimization problem:

$$(P) \begin{cases} \max_{\mathbf{x}} & \mathbf{x}^H \boldsymbol{\Phi}(\mathbf{x}) \mathbf{x} \\ \text{s.t.} & \|\mathbf{x} - \mathbf{x}_0\|_\infty \leq \epsilon \\ & |\mathbf{x}(k)| = 1/\sqrt{N_T N} \end{cases} \quad (2.5)$$

where  $\boldsymbol{\Phi}(\mathbf{x})$  is the SINR matrix. As shown in [15], the positive-semidefinite SINR matrix can be given as:  $\boldsymbol{\Phi}(\mathbf{x}) = \mathbf{U}(\theta_0)^H [\boldsymbol{\Sigma}(\mathbf{x}) + \mathbf{I}]^{-1} \mathbf{U}(\theta_0)$ . Note that the similarity constraint can be rewritten as:  $\arg \mathbf{x}(k) \in [\gamma_k, \gamma_k + \delta]$ , where  $\gamma_k = \arg \mathbf{x}_0(k) - \arccos(1 - \epsilon^2/2)$ ,  $\delta = 2 \arccos(1 - \epsilon^2/2)$ , and  $0 \leq \epsilon \leq 2$ . If  $\epsilon = 0$ , the waveform  $\mathbf{x}$  will be identical to the reference waveform  $\mathbf{x}_0$ . On the other hand, if  $\epsilon = 2$ , there will be no SC and the problem will have only a CMC.

In the existing literature [15, 16], the dependence of  $\boldsymbol{\Phi}(\mathbf{x})$  on the waveform  $\mathbf{x}$  has been resolved iteratively assuming  $\boldsymbol{\Phi}(\mathbf{x}) = \boldsymbol{\Phi}$  for a fixed  $\mathbf{x}$  and repeatedly optimizing  $\mathbf{x}$  with a new  $\boldsymbol{\Phi}$  till convergence. A key recent example is the sequential optimization algorithm (SOA) of Cui *et al* [15]. Nevertheless, even for a fixed  $\boldsymbol{\Phi}$ , the optimization of  $\mathbf{x}$  presents a hard non-convex problem, most popular solutions of which involve SDR with randomization [17, 18, 19, 15].

## 2.3 Methods, Assumptions, and Procedures

### 2.3.1 Overview of Contribution

To overcome the challenges mentioned above, this work develops a new algorithm for MIMO waveform design which jointly enforces CMC and SC. Specifically, this work makes the following contributions:

- **SQR: A new tractable analytical framework for waveform design that jointly enforces both CMC and SC.** In contrast to existing work, which relies on SDR with randomization and its extensions [17, 18, 19, 15, 20], our approach involves solving a sequence of convex problems (each a QCQP) such that in each iteration of the sequence the designed waveform satisfies the similarity constraint. Constant modulus is successively achieved at convergence, hence the method is called – Successive QCQP Refinement (SQR). No randomization is needed in our algorithm, which in turn also leads to significantly reduced computational complexity.
- **Analysis of the SQR based algorithm.** We formally prove that the SINR resulting from the proposed successive QCQP solution is non-decreasing in each step and converges (see [21]).
- **Extensions of SQR to incorporate spectral interference constraint and to deal with joint optimization of the waveform and the receive filter.** The proposed SQR can easily incorporate the practical interference constraints jointly with CMC and SC since the spectral interference constraint is modeled as a convex quadratic constraint [22, 23] and the SQR already relies on solving a QCQP. This work also develops the joint optimization of the transmit waveform and the receive filter as an extension of the proposed SQR. We solve the fractional quadratic optimization problem with the CMC and the SC using the parametric programming approach.

### 2.3.2 Successive QCQP Refinement

The optimization problem in (2.4) can be relaxed to the following convex optimization problem (*CP*):

$$(CP) \begin{cases} \max_{\mathbf{x}} & \mathbf{x}^H \mathbf{Q} \mathbf{x} \\ \text{s.t.} & |\mathbf{x}(k)|^2 \leq 1/(N_T N) \\ & a_k \text{Re}(\mathbf{x}(k)) + b_k \text{Im}(\mathbf{x}(k)) \geq c_k \end{cases} \quad (2.6)$$

where  $\mathbf{Q} = (\Phi - \lambda \mathbf{I})$  while the parameters  $a_k$ ,  $b_k$  and  $c_k$  represents the line that intersects with the constant modulus at the interval  $[\gamma_k, \gamma_k + \delta]$ . This relaxation becomes closer to (*NC*) as the value of  $\delta$  becomes smaller. For instance, if  $\delta = \frac{\pi}{2}$ , then the feasible value of  $|\mathbf{x}(k)|$  lies between  $\frac{1}{\sqrt{2}}$  and 1. Therefore, this property can be used to make  $|\mathbf{x}(k)|$  approach 1 by iteratively reducing  $\delta$ .

Furthermore, the problem *CP* can be converted to the following problem with *real* variables [24]:

$$\begin{cases} \max_{\mathbf{v}} & \mathbf{v}^T \mathbf{S} \mathbf{v} \\ \text{s.t.} & \mathbf{v}^T \mathbf{E}_k \mathbf{v} \leq 1/(N_T N), \quad k = 1, 2, \dots, N_T N \\ & \mathbf{A} \mathbf{v} \succeq \mathbf{c} \end{cases} \quad (2.7)$$

where:

$$\mathbf{S} = \begin{bmatrix} \text{Re } \mathbf{Q} & -\text{Im } \mathbf{Q} \\ \text{Im } \mathbf{Q} & \text{Re } \mathbf{Q} \end{bmatrix}, \quad (2.8)$$

$$\mathbf{v} = [\text{Re}(\mathbf{x}^T) \text{Im}(\mathbf{x}^T)]^T, \quad \mathbf{c} = \frac{1}{\sqrt{N_T N}} [1 \quad 1 \quad \dots \quad 1]^T,$$

$$\mathbf{A}(i, j) = \begin{cases} a_k & \text{if } i = j = k, \\ b_k & \text{if } i = k, \text{ and } j = k + N_T N, \\ 0 & \text{Otherwise.} \end{cases} \quad \mathbf{E}_k(i, j) = \begin{cases} 1 & \text{if } i = k, \text{ and } j = k + N_T N, \\ 0 & \text{Otherwise.} \end{cases}$$

Problem (2.7) is a real convex quadratically constrained quadratic program (QCQP), which can be easily converted to second order cone program (SOCP) [25][26] and solved efficiently [26, 27].

## Successive QCQP Refinement- Binary Search (SQR-BS) Algorithm

Consider the following problem:

$$(RC^{(n)}) \begin{cases} \max_{\mathbf{v}} & \mathbf{v}^T \mathbf{S} \mathbf{v} \\ \text{s.t.} & \mathbf{v}^T \mathbf{E}_k \mathbf{v} \leq 1/(N_T N), \\ & k = 1, 2, \dots, N_T N \\ & \mathbf{A}_n \mathbf{v} \succeq \mathbf{c} \\ & \mathbf{v}^{(n-1)T} \mathbf{P} \mathbf{v} \geq \mathbf{v}^{(n-1)T} \mathbf{P} \mathbf{v}^{(n-1)} \end{cases} \quad (2.9)$$

where  $\mathbf{v}^{(n-1)}$  is the optimal solution of  $RC^{(n-1)}$ ,  $\mathbf{S}$  is negative-semidefinite, while  $\mathbf{P} = \mathbf{S} + \lambda \mathbf{I}$  is positive definite. Note that, the SINR value of the  $n$ -th refinement is give as  $SINR^n = \mathbf{v}^{(n)T} \mathbf{P} \mathbf{v}^{(n)}$ .

At  $n = 0$ ,  $\mathbf{A}_0$  is chosen such that  $\arg \mathbf{x}(k) \in [\gamma_k, \gamma_k + \delta]$  as follows:

$$\mathbf{A}_0(i, j) = \begin{cases} \frac{\cos(\arg \mathbf{x}_0(k))}{\cos(\delta/2)} & \text{if } i = j = k, k = 1, 2, \dots, N_T N \\ \frac{\sin(\arg \mathbf{x}_0(k))}{\cos(\delta/2)} & \text{if } i = k, \text{ and } j = k + N_T N, \\ 0 & \text{Otherwise.} \end{cases}$$

which represents the straight line in Fig. 2.1 (a). Denote the solution of  $RC^{(0)}$  by  $\mathbf{v}^{(0)}$  and denote the complex solution of  $CP$  by  $\mathbf{x}^{(0)}$ . In this case, there will be two possibilities:

1. If  $\arg \mathbf{x}^{(0)}(k) \geq \gamma_k + \delta/2$ , we set the new SC as  $[\gamma_k + \delta/2, \gamma_k + \delta]$ , i.e, the new constraint angles  $\gamma_k^{(1)} = \gamma_k + \delta/2$  and  $\delta^{(1)} = \delta/2$ .
2. If  $\arg \mathbf{x}^{(0)}(k) < \gamma_k + \delta/2$ , then we set the new SC as  $[\gamma_k, \gamma_k + \delta/2]$ , i.e, the new constraint angles  $\gamma_k^{(1)} = \gamma_k$  and  $\delta^{(1)} = \delta/2$ .

In other words, the feasible SC interval is reduced to half according to the location of  $\arg \mathbf{x}^{(0)}(k)$ . In the next refinement we solve  $RC^{(1)}$  same as problem  $RC^{(0)}$  but with the new SC  $([\gamma_k^{(1)}, \gamma_k^{(1)} + \delta^{(1)}])$ . Continuing in the same fashion for  $RC^{(n)}$ ,  $n = 2, 3, \dots, F$ , the interval  $([\gamma_k^{(n)}, \gamma_k^{(n)} + \delta^{(n)}])$  will get smaller and smaller ( $\delta^{(n)} = \delta/2^n$ ) and eventually the modulus of  $\mathbf{x}^{(n)}(k)$  will converge to one, as illustrated in Fig. 2.1. This is similar to a binary search for  $\mathbf{x}^{(n)}(k)$ . The general form of  $\mathbf{A}_n$  is given by

$$\mathbf{A}_n(i, j) = \begin{cases} \frac{\cos(\gamma_k^{(n)} + \delta/2^n)}{\cos(\delta/2^n)} & \text{if } i = j = k, \\ \frac{\sin(\gamma_k^{(n)} + \delta/2^n)}{\cos(\delta/2^n)} & \text{if } i = k, \text{ and } j = k + N_T N, \\ 0 & \text{Otherwise.} \end{cases} \quad (2.10)$$

The SINR of the SQR algorithm is non-decreasing with each refinement unlike the SOA1 algorithm found in [15, 20] and also converges as shown in the following lemmas. For proofs of all lemmas in this report, please refer [?].

**Lemma 2.3.1.** *Let  $\mathbf{v}^{(n-1)}$  and  $\mathbf{v}^{(n)}$  be the optimal solutions of  $RC^{(n-1)}$  and  $RC^{(n)}$ , respectively. then:  $SINR^{n-1} = \mathbf{v}^{(n-1)T} \mathbf{P} \mathbf{v}^{(n-1)} \leq \mathbf{v}^{(n)T} \mathbf{P} \mathbf{v}^{(n)} = SINR^n$ . In other words, the sequence  $\{SINR^n\}_{n=0}^\infty$  is non-decreasing.*

**Lemma 2.3.2.** *The sequence  $SINR^n$  converges to a finite value  $SINR^*$ .*

## Successive QCQP Refinement - Non-Decreasing (SQR-ND) Algorithm

We propose an adjustment to the refinement part of SQR-BS which guarantees a non-decreasing SINR even if it is combined with sequential updates of  $\mathbf{x}$  and  $\Phi(\mathbf{x})$ . Furthermore, another advantage of this new modification is an easier calculation for the feasible region when introducing an interference constraint. The new algorithm is called SQR non-decreasing (SQR-ND). The affine constraint in the  $n^{th}$  refinement is given by:

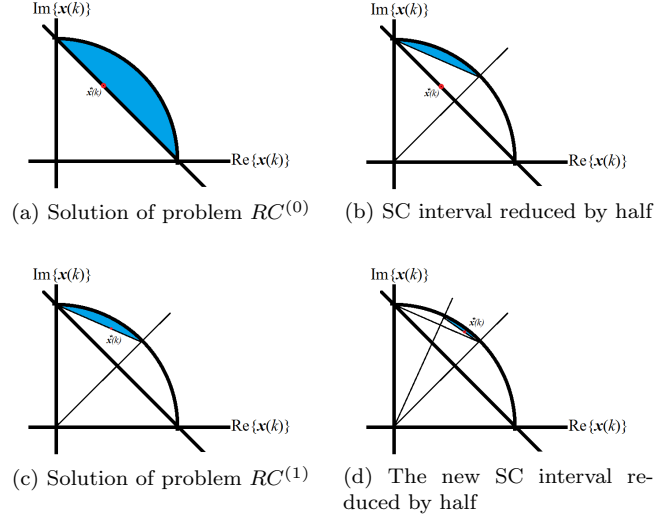


Figure 2.1: Illustration of the successive approximation of problem (2.5): (a) The convex hull of problem (2.5) is the blue area. (b) The solution point of the convex problem (2.6) in red. Now, we consider only the upper half of the similarity constraint and solve again. (c) Sconced refinement (d) Third refinement, here solution in the third refinement is very close to unity.

$$\mathbf{A}_n(i, j) = \begin{cases} \frac{\cos(\arg \mathbf{x}^{(n-1)}(k))}{\cos(\delta/2)} & \text{if } i = j = k, \\ \frac{\sin(\arg \mathbf{x}^{(n-1)}(k))}{\cos(\delta/2)} & \text{if } i = k, \text{ and } j = k + N_T N, \\ 0 & \text{Otherwise.} \end{cases}$$

with  $\mathbf{x}^{(0)}$  being any feasible point and  $\mathbf{x}^{(n-1)}$  is the complex version of  $\mathbf{v}^{(n-1)}$ . In this algorithm, the set of affine constraints  $\mathbf{A}_n \mathbf{v}$  rotate according to  $\mathbf{v}^{(n-1)}$ , which may violate the SC. Therefore, two sets of affine constraints has been introduced to ensure SC is satisfied. The matrices for these additional constraints are given as:

$$\mathbf{B}_{\pm}(i, j) = \begin{cases} \pm -\sin(\arg \mathbf{x}_0(k)) - \tan(\delta/2) \cos(\arg \mathbf{x}_0(k)) & \\ \text{if } i = j = k, & \\ \pm \cos(\arg \mathbf{x}_0(k)) - \tan(\delta/2) \sin(\arg \mathbf{x}_0(k)) & \\ \text{if } i = k, \text{ and } j = k + N_T N, & \\ 0, \text{ Otherwise.} & \end{cases}$$

Finally, the refinement optimization problem is rewritten as:

$$(RCND^{(n)}) \left\{ \begin{array}{l} \max_{\mathbf{v}} \quad \mathbf{v}^T \mathbf{S} \mathbf{v} \\ \text{s.t.:} \quad \mathbf{v}^T \mathbf{E}_k \mathbf{v} \leq 1/(N_T N), \\ \quad \quad \quad k = 1, 2, \dots, N_T N \\ \quad \quad \quad \mathbf{A}_n \mathbf{v} \succeq \mathbf{c} \\ \quad \quad \quad \mathbf{B}_+ \mathbf{v} \preceq \mathbf{0} \\ \quad \quad \quad \mathbf{B}_- \mathbf{v} \preceq \mathbf{0} \end{array} \right. \quad (2.11)$$

In particular, let  $\mathbf{x}^{(n-1)}$  be the complex version of the optimal solution to  $RCND^{(n-1)}$ , i.e.  $\mathbf{v}^{(n-1)} = [\text{Re}(\mathbf{x}^{(n-1)T}) \text{Im}(\mathbf{x}^{(n-1)T})]^T$ , the SQR-ND adjusts the affine constraints so that the feasible set of next refinement will include what we call as the *constant modulus version* of  $\mathbf{x}^{(n-1)}$  given by  $\mathbf{x}_{(n-1)} = \exp(j \arg(\mathbf{x}^{(n-1)})) / \sqrt{N_T N}$ . Convergence is then guaranteed which establishes that the SINR sequence that results by using the solution of each refinement, is in fact non-decreasing and converges.

**Lemma 2.3.3.** Let  $\mathbf{x}^{(n-1)}$  and  $\mathbf{x}^{(n)}$  be the complex version of the optimal solutions  $\mathbf{v}^{(n-1)}$  and  $\mathbf{v}^{(n)}$ , respectively, where  $n$  is the refinement index. Define  $\text{SINR}^n = \mathbf{x}^{(n)H} \mathbf{Q} \mathbf{x}^{(n)}$  then:  $\text{SINR}^{n-1} = \mathbf{x}^{(n-1)H} \mathbf{Q} \mathbf{x}^{(n-1)} \leq \mathbf{x}^{(n)H} \mathbf{Q} \mathbf{x}^{(n)} = \text{SINR}^n$ . In other words, the sequence  $\{\text{SINR}^n\}_{n=0}^{\infty}$  is non-decreasing over refinements.

**Lemma 2.3.4.** The sequence  $\text{SINR}^n$  defined converges to a finite value  $\text{SINR}^*$ .

**Lemma 2.3.5.** If the solution converges to constant modulus, then the sequence  $\text{SINR}^n$  is non-decreasing over iterations and converges.

## SQR-ND with Interference Constraint

A major advantage of our proposed convex formulation is the simplicity of adding a new convex interference constraint. However, since the algorithm must be solved in several refinements, we need to ensure that the feasible set is not empty before each refinement. Nevertheless, in the case of interference constraint, we have a quadratic constraint that is shaped by  $\mathbf{R}_I$ . Fortunately, we can compute the feasibility of the problem once and ensure that the problem will be feasible in each refinement. For more details please refer to paper [21].

### 2.3.3 Joint Optimization of Waveform and Receive Filter

In this section, as an extension of the proposed SQR, we develop the joint optimization of the transmit waveform and the receive filter based on the SQR and using the parametric programming approach. First, recall the joint optimization problem of  $\mathbf{x}$  and  $\mathbf{w}$  (2.4). It can be rewritten as an optimization problem of  $\mathbf{x}$  for a fixed  $\mathbf{w}$ ,

$$\begin{cases} \max_{\mathbf{x}} & \frac{\mathbf{x}^H \boldsymbol{\Sigma}_t(\mathbf{w}) \mathbf{x}}{\mathbf{x}^H \boldsymbol{\Sigma}_I(\mathbf{w}) \mathbf{x}} \\ \text{subject to} & \|\mathbf{x} - \mathbf{x}_0\|_{\infty} \leq \epsilon \\ & |\mathbf{x}(k)| = 1/\sqrt{N_T N} \end{cases} \quad (2.12)$$

where  $\boldsymbol{\Sigma}_t(\mathbf{w}) = \sigma \mathbf{U}^H(\theta_0) \mathbf{w} \mathbf{w}^H \mathbf{U}(\theta_0)$  and  $\boldsymbol{\Sigma}_I(\mathbf{w}) = \sum_{k=1}^K I_k \mathbf{U}^H(\theta_k) \mathbf{w} \mathbf{w}^H \mathbf{U}(\theta_k) + \mathbf{I}$

Now we discuss how to solve the fractional optimization problem (2.12). The objective function of (2.12) is a quadratic fractional function with a positive denominator since  $\boldsymbol{\Sigma}_I(\mathbf{w})$  is positive definite. Previous studies of nonlinear fractional programming [28, 29, 30] have shown that the quadratic fractional programming problem (2.12) can be converted to the following parametric programming problem.

$$\begin{cases} \max_{\mathbf{x}, \alpha} & \mathbf{x}^H \boldsymbol{\Sigma}_t(\mathbf{w}) \mathbf{x} - \alpha (\mathbf{x}^H \boldsymbol{\Sigma}_I(\mathbf{w}) \mathbf{x}) \\ \text{s.t.} & |\mathbf{x}(k)| = 1/\sqrt{N_T N} \\ & \|\mathbf{x} - \mathbf{x}_0\|_{\infty} \leq \epsilon \end{cases} \quad (2.13)$$

$\alpha$  and  $\mathbf{x}$  in (2.13) can be alternately optimized through the generalized Newton method [30]. Specifically, for given  $\mathbf{x}_k$ ,  $\alpha_{k+1}$  can be updated by

$$\alpha_{k+1} = \alpha_k - \frac{\mathbf{x}_k^H \boldsymbol{\Sigma}_t(\mathbf{w}) \mathbf{x}_k - \alpha_k (\mathbf{x}_k^H \boldsymbol{\Sigma}_I(\mathbf{w}) \mathbf{x}_k)}{-\mathbf{x}_k^H \boldsymbol{\Sigma}_I(\mathbf{w}) \mathbf{x}_k} \quad (2.14)$$

$$= \frac{\mathbf{x}_k^H \boldsymbol{\Sigma}_t(\mathbf{w}) \mathbf{x}_k}{\mathbf{x}_k^H \boldsymbol{\Sigma}_I(\mathbf{w}) \mathbf{x}_k} \quad (2.15)$$

Then  $\mathbf{x}_{k+1}$  can be obtained by solving (2.13) for given  $\alpha_{k+1}$ . The properties of convergence and non-decreasing cost function of the parametric programming have already been proven in the literature [28, 31]. That is, the sequence of the objective function of (2.13) is a strictly non-decreasing sequence and converges to the maximum value of the objective function of (2.12).

Now we focus on solving (2.13) to obtain  $\mathbf{x}$  for a fixed  $\alpha$ . The parametric programming problem (2.13) is equivalent to the following problem.

$$\begin{cases} \max_{\mathbf{x}} & \mathbf{x}^H \Sigma_t(\mathbf{w})\mathbf{x} - \alpha(\mathbf{x}^H \Sigma_I(\mathbf{w})\mathbf{x}) \\ \text{s.t.} & |\mathbf{x}(k)| = \frac{1}{\sqrt{N_T N}}, \quad k = 1, \dots, N_T N \\ & \arg \mathbf{x}(k) \in [\gamma_k, \gamma_k + \delta], \quad k = 1, \dots, N_T N \end{cases} \quad (2.16)$$

where  $\gamma_k$  and  $\delta$  define the equivalent similarity constraint and are given by

$$\gamma_k = \arg \mathbf{x}_0(k) - \arccos(1 - \epsilon^2/2) \quad (2.17)$$

$$\delta = 2 \arccos(1 - \epsilon^2/2) \quad (2.18)$$

Note that (2.16) can be easily converted to the form of (2.6) and solved by the proposed SQR method. The proposed algorithm optimizes the transmit waveform  $\mathbf{x}$  and the receiver filter  $\mathbf{w}$  alternately. The optimization problem we solve is (2.4) with respect to  $\mathbf{x}$  and  $\mathbf{w}$ . The procedure is following: First we obtain the optimal filter  $\mathbf{w}$  for a given  $\mathbf{x}$ . Then for a given  $\mathbf{w}$ , we solve (2.12) and obtain the optimal  $\mathbf{x}$  by alternately updating  $\mathbf{x}$  and  $\alpha$ . During this process,  $\alpha$  can be obtained by Eq. (2.15) for a given  $\mathbf{x}$ . Then for a given  $\alpha$ ,  $\mathbf{x}$  can be updated by solving (2.13) via the SQR method which involves the successive refinements of the constraint set to achieve the constant modulus constraint.

## 2.4 Results and Discussions

### 2.4.1 Experimental Setup and Methods Compared

The number of transmit and receive antennas are  $N_T = 4$  and  $N_R = 8$  elements, respectively. For the reference signal  $\mathbf{x}_0$ , we considered the orthogonal linear frequency modulation (LFM) waveform. It can be defined by the space-time waveform matrix:

$$\mathbf{X}_0(k, n) = \frac{\exp\{j2\pi k(n-1)/N\} \exp\{j\pi(n-1)^2/N\}}{\sqrt{N N_T}} \quad (2.19)$$

where  $k = 1, \dots, N_T$  and  $n = 1, \dots, N$ . The reference waveform vector  $\mathbf{x}_0$  is the generated by stacking the column of  $\mathbf{X}_0$ . In section 2.4.2, we compare our algorithms (both SQR-BS and SQR-ND) to SDR with randomization method for a fixed SINR matrix  $\Phi$ , i.e. absence of signal dependent clutter. Then we compare our algorithm to the Sequential Optimization Algorithm 1 and 2 (SOA1 and SOA2), i.e. the sequential SDR and randomization approach of [15]. In both these scenarios, the number of randomization trials used was 20000, as in [15] and our proposed SQR algorithms involved four refinement steps, i.e.  $F = 4$ . The noise variance is  $\sigma_n = 0$  dB. In section 2.4.2, we introduce a spectral interference constraint and compare our method to the recently developed CRCO in [22].

### 2.4.2 Experimental Evaluation

#### Waveform design with Constant Modulus and Similarity Constraint

Our set up involves a target located at an angle  $\theta_0 = 15^\circ$  with a reflecting power of  $|\alpha_0|^2 = 10$  dB.

Figure 2.2 shows the SINR behavior of the output waveform versus  $\epsilon$  the similarity constraint parameter – see (2.5). Clearly, the proposed SQR-BS and SQR-ND outperform the SDR with randomization and the performance gap increases as  $\epsilon$  increases. The SQR-BS has higher SINR values particularly when the similarity parameter become large.

Moreover, the proposed algorithms achieve a higher SINR value when the similarity constraint is strong, i.e. lower values of  $\epsilon$ , even with one or two refinements. This is verified in Fig. 2.3, which further reveals that SQR-BS with two refinements achieves better SINR than SDR with randomization for  $\epsilon \leq 0.88$  and for  $\epsilon \leq 0.43$  in case of one refinement. SQR-ND is always better than SDR with randomization for  $F = 2$  refinements. Examining the performance of SQR-BS and SQR-ND for varying  $F$  is insightful from a complexity standpoint.

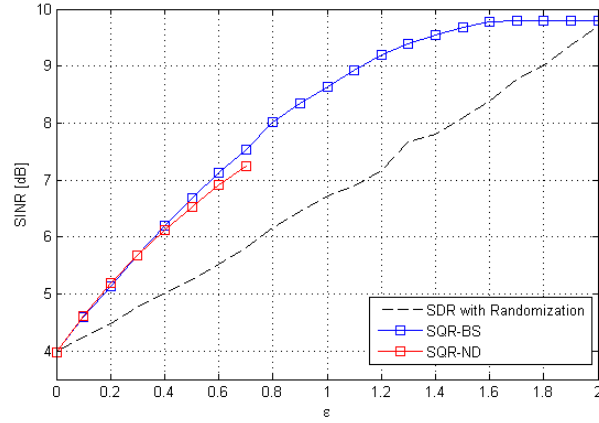


Figure 2.2: The SINR of the optimal waveform design versus the similarity parameter  $\epsilon$  for constant SINR matrix ( signal independent clutter). SQR-BS and SQR-ND are compared against SDR with randomization [32, 15].

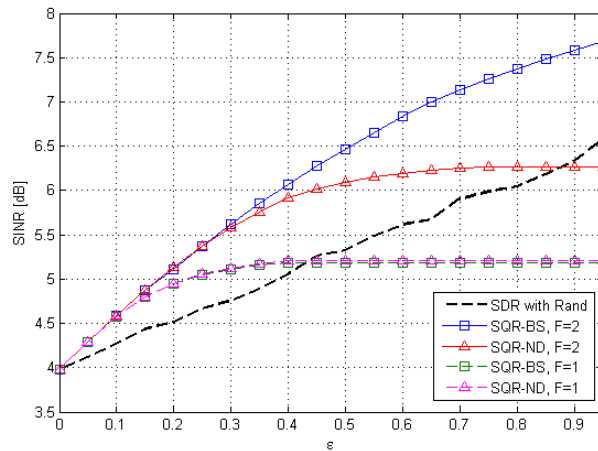


Figure 2.3: The SINR of the optimal waveform design versus the similarity parameter  $\epsilon$  for constant SINR matrix (no signal dependent clutter). SQR-BS and SQR-ND are compared against the SDR with randomization.

Table 2.1: Computational Complexity of One iteration

Method	Order of Complexity	Sim. Time (sec)
SOA1[15]	$\mathcal{O}(N_T^{3.5} N^{3.5}) + \mathcal{O}(LN_T^2 N^2)$	11.2 s
SOA2[15]	$\mathcal{O}(N_T^{3.5} N^{3.5}) + \mathcal{O}(LN_T^2 N^2)$	10 s
SQR-BS	$\mathcal{O}(FN_T^{3.5} N^{3.5})$	6.3 s
SQR-ND	$\mathcal{O}(FN_T^{3.5} N^{3.5})$	7.4 s

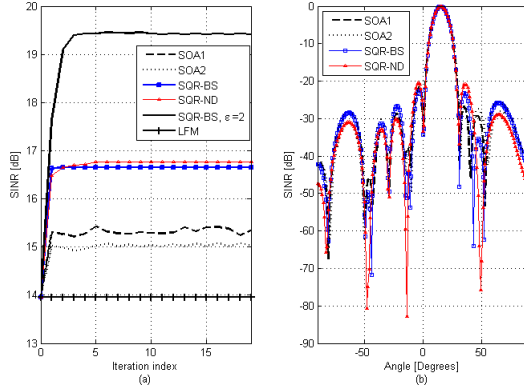


Figure 2.4: (a) The SINR of the optimal waveform design in each iteration and in (b) the beampattern  $P(\theta)$  for SOA1, SQR-BS and SQR-ND algorithms with  $\epsilon = 0.5$  for all of them.

### Waveform design with Constant Modulus and Similarity Constraint Under Signal Dependent Clutter

For consistency with the results reported in [15], all parameter choices are as in [15] while comparing SQR against with SOA1 and SOA2 [15, 20] in the presence of clutter. The target is located at an angle  $\theta_0 = 15^\circ$  with a reflecting power of  $|\alpha_0|^2 = 20$  dB and three fixed interferences located at  $\theta_1 = -50^\circ$ ,  $\theta_2 = -10^\circ$  and  $\theta_3 = 40^\circ$  reflecting a power of  $|\alpha_1|^2 = |\alpha_2|^2 = |\alpha_3|^2 = 30$  dB. Table 2.1 shows the computational complexity and the simulation time of the different methods. To show the suppression capability of the resulting waveform, the beam pattern is shown in Fig. 2.4 (b). The SQR optimized beam pattern resulting from the proposed algorithms exhibits much better suppression performance at  $\theta = -50$  and  $\theta = -10$  when compared to SOA1.

A plot of the final SINR value (at convergence) vs. the similarity constraint parameter  $\epsilon$  for sequential SQR-BS and SOA1 is shown in Fig. 2.5. Remarkably, the SOA1 increases approximately linearly with  $\epsilon$  while the SQR-BS exhibits a superlinear increase.

### Waveform design with SC, CMC and Spectral Interference Constraint

First, we will compare our method with only CMC to a state of the art recent method that uses an energy constraint: SQR-BS for Cognitive Radar Code Optimization (CRCO1) found in [22] for SISO case  $N_T = N_R = 1$  and no signal dependent interference to obtain some insight about how much loss is incurred by incorporating the CMC. In this case, we use the following SINR matrix  $\Phi = \sigma_0 \mathbf{I} + \sum_{k=1}^{K_J} \frac{\sigma_{J,k}}{\Delta f_J^k} \mathbf{R}_J^k$ , where  $\mathbf{R}_I = \sum_{k=1}^K w_k \mathbf{R}_I^k$ ,  $\sigma_0 = 0$  dB is the noise level,  $K_J = 2$  is the number of active unlicensed radiators or jammers,  $\sigma_{J,k} = 50$  dB for  $k = 1, 2$  is the energy of the  $k$ -th active unlicensed radiators using the normalized frequency band  $B_J^k = [f_{J,1}^k, f_{J,2}^k]$  and  $\Delta f_J^k = f_{J,2}^k - f_{J,1}^k$  is the bandwidth used by the  $k$ -th coexisting radiator. Furthermore, the normalized frequency band of the first and second unlicensed radiator are  $B_J^1 = [0.2, 0.22]$  and  $B_J^2 = [0.6, 0.635]$ , respectively. For  $\mathbf{R}_I$  we used  $B^1 = [f_1^1, f_2^1] = [0.05, 0.08]$ ,  $B^2 = [f_1^2, f_2^2] = [0.4, 0.435]$ ,  $w_1 = w_2 = 1$  and  $E_I = 0.005$ . Fig. 2.6 shows the the Energy Spectral Density (ESD) of the proposed algorithm SQR-ND-Int with CMC against CRCO1 as well as the reference LFM waveform. Since CRCO1 does not enforce CMC,

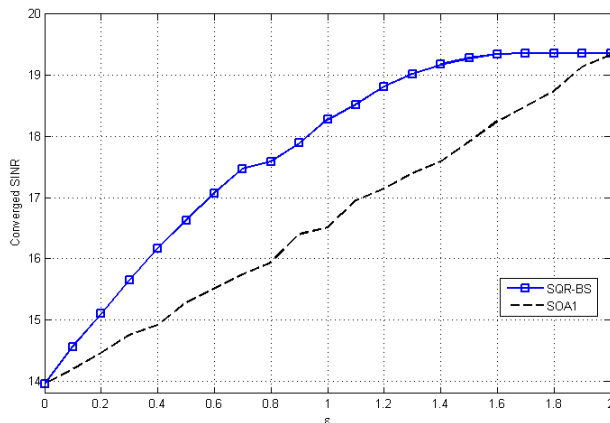


Figure 2.5: The converged SINR values of SQR-BS and SOA1 vs.  $\epsilon$

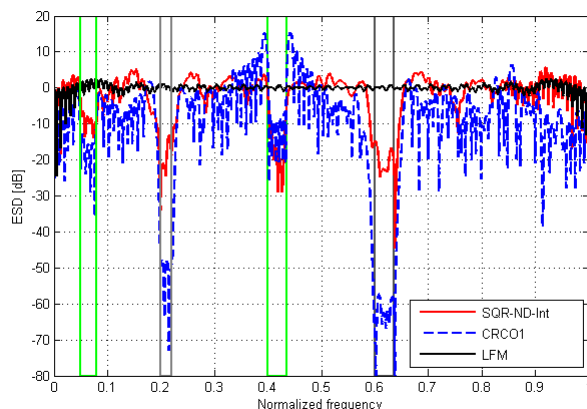


Figure 2.6: The plot ESD in dB for: 1) reference waveform  $\mathbf{x}_0$  in black dashed line, 2) the output waveform  $\mathbf{x}^*$  using CRCO1 in blue dotted line, 3) the output waveform using SQR-ND-Int in red.

it manages to reduce the interference level in the unlicensed band (shown between the gray vertical lines) by a larger amount although both SQR-ND-Int and CRCO1 achieve the same interference levels in the licensed band. The SINR values corresponding to different waveforms are -0.0007 dB, -0.0262 dB and -0.5122 dB for the CRCO1, SQR-ND-Int and the LFM waveforms, respectively. In summary, a relatively small loss (against CRCO1) in SINR value is seen via the proposed SQR-ND-Int even as CMC is captured simultaneously with interference constraint and in an analytically tractable manner.

For the MIMO scenario, we include the signal dependent clutter, therefore, the signal waveform design should reduce both the spectral coexistence interference and reject clutter. In this simulation, we assumed a LFM pulse with  $N = 120$  and MIMO antennas with  $N_T = 2$  and  $N_R = 4$ . We assume three clutter interferences with the same power and amplitudes as in Section 2.4.2. The covariance matrix  $\mathbf{M}$  of the signal-independent interference has been modeled as the MIMO generalization of [23] as  $\mathbf{M} = \sum_{k=1}^K \frac{\sigma_{I,k}}{\Delta f_k} \mathbf{U}(\psi_k) \mathbf{R}_I^k \mathbf{U}^H(\psi_k)$ , where  $\psi_k$  is the angle of the  $k$ -th radiator,  $K = 2$  is the number of licensed radiators,  $\psi_1 = 30^\circ$  while  $\psi_2 = -20^\circ$ ,  $\sigma_{I,k} = 10$  dB for  $k = 1, 2$  is the energy of the  $k$ -th coexisting radiator using the normalized frequency band  $B^k = [f_1^k, f_2^k]$  and  $\Delta f_k = f_2^k - f_1^k$  is the bandwidth used by the  $k$ -th coexisting radiator. Furthermore, the normalized frequency band of the first and second coexisting radiator are  $B^1 = [0.05, 0.08]$  and  $B^2 = [0.4, 0.435]$ , respectively. As expected, the optimized waveforms from the proposed algorithm reduce the interference in the specified frequency bands.

## Joint Optimization of Transmit Waveform and Receive Filter

In Fig. 2.7a and Fig. 2.7b, we compare our joint optimization algorithm against the previous waveform design algorithm called sequential optimization algorithm (SOA) proposed by Cui *et al.* in the sense of SINR and beampattern. In particular, we compare SOA2 in [15] since SOA2 solves the same fractional quadratic optimization problem under the constant modulus constraint and the similarity constraint by using semidefinite relaxation (SDR) with randomization. For SOA2, the number of randomization trials is 20,000 as in [15].

Fig. 2.7a shows the SINR improvement in each iteration of  $\mathbf{x}$  and  $\mathbf{w}$  for SOA2 and the proposed algorithm. It is shown that the proposed algorithm achieves a value of SINR 1.2 dB higher than SOA2. Regarding convergence rate, the proposed algorithm converges after 8 iterations while the SINR value of SOA2 still fluctuates after 20 iterations. Further, the proposed method shows the non-decreasing SINR whereas the SINR of the SOA2 is not monotonically increasing.

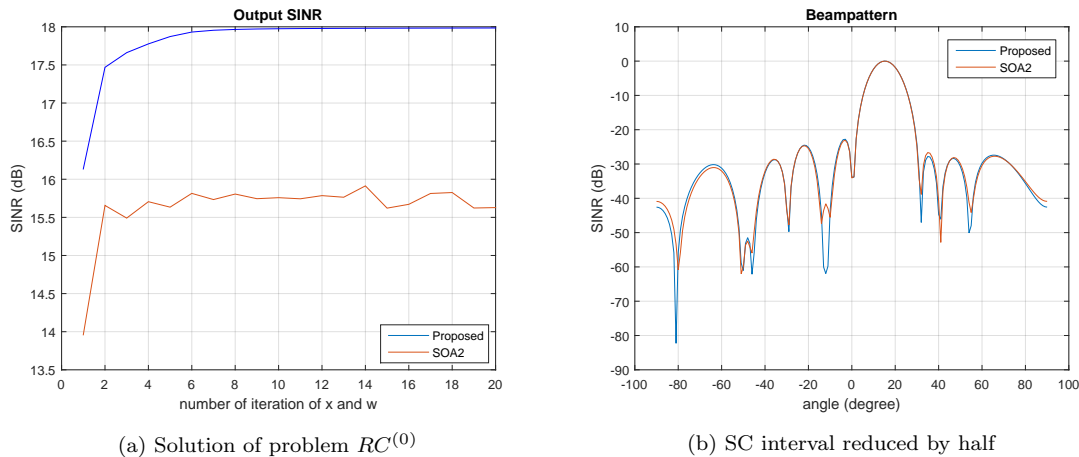


Figure 2.7: (a) The SINR of the proposed algorithm and SOA2 with  $\epsilon = 0.8$  vs. the number of iteration. (b) Beampattern of the estimated waveform of the proposed algorithm and SOA2 with  $\epsilon = 0.8$ .

## 2.5 Conclusions

Our work achieves tractable waveform design for MIMO radar in the presence of constant modulus and similarity constraints. The central idea of our analytical contribution is to successively refine and achieve constant modulus (at convergence), while solving a sequence of quadratically constrained quadratic programs, such that each optimization in the sequence satisfies a similarity constraint. We also extend the proposed SQR algorithm to the joint optimization problem of the transmit waveform and the receive filter using the parametric programming approach. We show this approach can achieve superior SINR and beam pattern with desirable suppression results against state of the art, remarkably at a lower computational cost.

## Chapter 3

# Tractable Transmit MIMO Beampattern Design Under a Constant Modulus Constraint

### 3.1 Summary

The management of the radar radiation power by shaping the beampattern has become crucial to efficiently utilize consumed energy, reduce interference and increase the probability of detection [33, 5].

Optimization of MIMO waveform to achieve the desired beampattern design has been a topic of much recent interest [34, 35, 36, 37, 38, 39, 11, 13, 12, 40, 41, 42, 43, 44, 45, 46, 47, 48, 49, 50, 51]. Some of these works focus on receive beampattern design [45, 46] while most others focus on the transmit beampattern [47, 48, 49, 50, 51]. In practice, the transmit beampattern is more difficult to design due to the requirement of a constant modulus constraint (CMC) on the radar transmit waveform, i.e. a constant envelop transmit signal [52].

The importance of the waveform CMC has been well documented and analyzed in terms of performance loss [52, 14, 16]. Most radar systems utilize non-linear power amplifiers which cannot be efficiently utilized without CMC. Specifically, the output of the amplifier will be a clipped version of the optimized waveform, which often leads to a significant degradation in the system performance.

Both narrowband and wideband MIMO transmit beampattern design under waveform CMC have been studied in [39, 13, 11, 51]. It is well-known that the problem of minimizing deviation of the designed beampattern vs. an idealized one subject to the constant modulus constraint (CMC) constitutes a hard non-convex problem. To ensure tractability, some existing approaches pursue relaxations of or approximations to the CMC. An exemplary approach in this category is [47, 51], where an approximation to constant modulus was pursued using the peak-to-average ratio (PAR) waveform constraint. While the CMC is not explicitly represented in the optimization process, the resulting solution is converted to the nearest constant modulus solution. This indirect approximation makes the problem more tractable, however, it degrades the design accuracy. Some recent efforts directly enforce CMC and hence lead to better performance. However, they involve computationally expensive procedures such as the gradient-based methods in [11] or Semidefinite Relaxation (SDR) with randomization [19, 17, 18]. Moreover, the design criterion of some of the recent work does not allow full control of power allocation such as [53] where the objective is to minimize radiation power in a few selected directions. An interesting recent advance that forces CMC for (narrowband) beampattern design has been proposed in [39] which sets up waveform design as a phase optimization problem and solves it using a typical iterative numerical method but with no known analytical guarantees of the resulting solution.

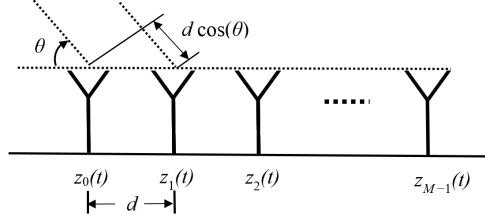


Figure 3.1: Configuration of ULA antenna

## 3.2 Introduction

### 3.2.1 System Model

Consider a *wideband* MIMO radar with a Uniform Linear Array (ULA) of  $M$  antennas and equal spacing distance of  $d$ , as shown in Fig. 3.1. The signal transmitted from the  $m$ -th element is denoted by  $z_m(t)$ . Let  $z_m(t) = x_m(t)e^{j2\pi f_c t}$  where  $x_m(t)$  is the baseband signal and  $f_c$  is the carrier frequency. We assume that the spectral support of  $x_m(t)$  is within the interval  $[-B/2, B/2]$  where  $B$  is the bandwidth in Hz. The sampled baseband signal transmitted by the  $m$ -th element is denoted by  $x_m(n) \triangleq x_m(t = nT_s)$ ,  $n = 0, \dots, N-1$  with  $N$  being the number of time samples and  $T_s = 1/B$  is the sampling rate. The discrete Fourier Transform (DFT) of  $x_m(n)$  is denoted by  $y_m(p)$  and it can be expressed as:

$$y_m(p) = \sum_{n=0}^{N-1} x_m(n) e^{-j2\pi \frac{np}{N}}, \quad p = -\frac{N}{2}, \dots, 0, \dots, \frac{N}{2} - 1 \quad (3.1)$$

According to [51], the discrete frequency beampattern in the far-field is given by:

$$P(\theta, p) = |\mathbf{a}^H(\theta, p) \mathbf{y}_p|^2 \quad (3.2)$$

where

$$\mathbf{a}(\theta, p) = [1 \quad e^{j2\pi(\frac{p}{NT_s} + f_c)\frac{d \cos \theta}{c}} \quad \dots \quad e^{j2\pi(\frac{p}{NT_s} + f_c)\frac{(M-1)d \cos \theta}{c}}]^T \quad (3.3)$$

and

$$\mathbf{y}_p = [y_0(p) \quad y_1(p) \quad \dots \quad y_{M-1}(p)]^T \quad (3.4)$$

Note that  $\mathbf{a}(\theta, p)$  is continuous in phase. It can be expressed as a discrete angle vector by dividing the interval  $[0^\circ, 180^\circ]$  to  $K$  angles. Using the same simplified notation found in [51], it can be written as:

$$\mathbf{a}_{kp} = \mathbf{a}\left(\theta_k, \frac{p}{NT_s}\right), \quad k = 1, 2, \dots, K \quad (3.5)$$

In this case, the beampattern can be given by the following discrete angle-frequency grid:

$$P_{kp} = |\mathbf{a}_{kp}^H \mathbf{y}_p|^2 = |\mathbf{a}_{kp}^H \mathbf{F}_p \mathbf{x}|^2 \quad (3.6)$$

where  $\mathbf{x} \in \mathbb{C}^{MN \times 1}$  is the concatenated  $MN \times 1$  vector i.e.  $\mathbf{x} = [\mathbf{x}_0^T \quad \mathbf{x}_1^T \quad \dots \quad \mathbf{x}_{M-1}^T]^T$  where  $\mathbf{x}_m = [x_m(0) \quad x_m(1) \quad \dots \quad x_m(N-1)]^T$  and  $\mathbf{F}_p$  is given by:

$$\mathbf{F}_p = \mathbf{e}_p \otimes \mathbf{I}_M \quad (3.7)$$

where  $\otimes$  is the Kronecker product,  $\mathbf{e}_p = [1 \quad e^{-j2\pi \frac{p}{N}} \quad \dots \quad e^{-j2\pi \frac{(N-1)p}{N}}]$  and  $\mathbf{I}_M$  is the  $M \times M$  identity matrix. The optimization problem can be formulated as the following matching problem:

$$\begin{cases} \min_{\mathbf{x}} & \sum_{k=1}^K \sum_{p=-\frac{N}{2}}^{\frac{N}{2}-1} [d_{kp} - |\mathbf{a}_{kp}^H \mathbf{F}_p \mathbf{x}|]^2 \\ \text{s.t.} & |\mathbf{x}| = \mathbf{1} \end{cases} \quad (3.8)$$

where  $d_{kp} \in \mathbb{R}$  is the desired beampattern and the constant modulus constraint ( $|\mathbf{x}| = \mathbf{1}$ ) implies that  $|x_m(n)| = 1$  for  $m = 0, 1, \dots, M$  and  $n = 0, 1, \dots, N$ . These constraints are non-convex, non-linear and it is well-known in the literature that (3.8) is a hard non-convex problem. *He et. al.* [51] proposed a solution to problem (3.8) by instead employing a peak-to-average ratio constraint. However, they used the cyclic algorithm [54, 55] to solve the unconstrained problem  $\min_{\mathbf{y}_p} \sum_{k=1}^K \sum_{p=-\frac{N}{2}}^{\frac{N}{2}-1} [d_{kp} - |\mathbf{a}_{kp}^H \mathbf{y}_p|]^2$  in the first stage and then in the second stage they aim to find the constant modulus approximation of the solution. The algorithm does not directly minimize the cost function under constant modulus constraint or any relaxed version thereof. In this paper, we propose a new solution that minimizes the cost function of interest by solving a sequence of problems under a relaxed convex constraint such that constant modulus is still achieved at convergence. The proposed new solution has the ability to break the computational cost-solution quality trade-off that has been demonstrated in past work such as SDR with randomization [17, 18, 19, 15] or the simulated annealing approach [51].

*Remark:* The problem formulation of narrowband null forming is a straight forward modification of the wideband case, and is covered in Section 3.3.2.

### 3.2.2 Problem Formulation

As shown in [51], it is more convenient to rewrite the objective function of eq. (3.8) as:

$$\sum_{k=1}^K \sum_{p=-\frac{N}{2}}^{\frac{N}{2}-1} |d_{kp} e^{j\phi_{kp}} - \mathbf{a}_{kp}^H \mathbf{F}_p \mathbf{x}|^2 \quad (3.9)$$

where  $\phi_{kp} = \arg\{\mathbf{a}_{kp}^H \mathbf{F}_p \mathbf{x}\}$ . Since  $\mathbf{x}$  is unknown,  $\phi_{kp}$  is also unknown for all values of  $k$  and  $p$ . In the existing literature [51, 54, 55], this problem has been resolved by an iterative method. This method minimizes eq. (3.9) by fixing the values of  $\{\phi_{kp}\}$  and minimizing w.r.t.  $\mathbf{x}$  and then fixing  $\mathbf{x}$  and minimizing w.r.t.  $\{\phi_{kp}\}$ . It has been shown that such an iterative method, ensures that the cost function is monotonically decreasing and converges to a finite value [51, 54, 55]. Therefore, we focus on solving the following constrained problem for fixed values of  $\{\phi_{kp}\}$ :

$$(P') \begin{cases} \min_{\mathbf{x}} & \sum_{k=1}^K \sum_{p=-\frac{N}{2}}^{\frac{N}{2}-1} |d_{kp} e^{j\phi_{kp}} - \mathbf{a}_{kp}^H \mathbf{F}_p \mathbf{x}|^2 \\ \text{s.t.} & |\mathbf{x}| = \mathbf{1} \end{cases} \quad (3.10)$$

Now, let us define the following:

$$\mathbf{A}_p = \begin{bmatrix} \mathbf{a}_{1p}^H \\ \vdots \\ \mathbf{a}_{Kp}^H \end{bmatrix}, \quad \mathbf{d}_p = \begin{bmatrix} d_{1p} e^{j\phi_{1p}} \\ \vdots \\ d_{Kp} e^{j\phi_{Kp}} \end{bmatrix}. \quad (3.11)$$

## 3.3 Methods, Assumptions, and Procedures

### 3.3.1 Overview of Contribution

The principal aim is to develop an algorithmic approach that can design constant modulus MIMO waveforms in a tractable manner while retaining high levels of performance in the sense of measures such as closeness to an idealized beampattern. As argued above, existing work invariably trades off performance vs. computation in a rigid manner. Specifically, this paper makes the following contributions:

- **Sequence of Closed Forms: A new algorithmic solution for both narrowband and wideband beampattern design under waveform CMC.** To overcome the challenges mentioned above, we develop a new algorithm for MIMO beampattern design that involves solving the hard non-convex problem of beampattern design using a sequence of convex equality constrained Quadratic Programs (QP), each of which has a closed form solution, such that constant

modulus is achieved at convergence. Because each QP in the sequence has a closed form, the proposed successive closed forms (SCF) algorithm has significantly lower complexity than competing methods that incorporate CMC. Moreover, the SCF algorithm can be used to minimize power in selected directions or to allow full control of the power allocation as in [51].

- **Convergence of the SCF Algorithm.** We formally prove that the sequence of cost functions representing deviation from the desired beampattern, that occurs in the proposed SCF algorithm is non-increasing, i.e. an improvement is obtained by solving each problem in the sequence. We further prove that the sequence of waveform solutions (via solving each QP) converges to constant modulus.
- **Properties of the SCF Solution.** We prove that the SCF solution satisfies the KarushKuhnTucker (KKT) conditions of the non-convex optimization problem, which are necessary conditions for optimality.
- **Experimental insights and validation.** Experimental validation is performed via numerical simulations. We considered two scenarios: 1) Narrowband null forming where the SCF algorithm shows significant power suppression in the desired directions. 2) Wideband beampattern design where the proposed SCF is shown to achieve a beampattern much closer to the ground truth unconstrained design against state of the art alternatives. In addition, the proposed SCF is robust to the presence of noise in the designed waveform, making it even more appealing from a practical standpoint.

### 3.3.2 Sequence of Closed Forms Solutions

The objective function of problem (3.10) can be rewritten in terms of  $\mathbf{A}_p$  and  $\mathbf{d}_p$  as:

$$\begin{aligned}
f(\mathbf{x}) &= \sum_p \|\mathbf{d}_p - \mathbf{A}_p \mathbf{F}_p \mathbf{x}\|_2^2 \\
&= \sum_p \mathbf{x}^H \mathbf{F}_p^H \mathbf{A}_p^H \mathbf{A}_p \mathbf{F}_p \mathbf{x} - \mathbf{d}_p^H \mathbf{A}_p \mathbf{F}_p \mathbf{x} - \mathbf{x}^H \mathbf{F}_p^H \mathbf{A}_p^H \mathbf{d}_p \\
&\quad + \sum_p \mathbf{d}_p^H \mathbf{d}_p \\
&= \mathbf{x}^H \left( \sum_p \mathbf{F}_p^H \mathbf{A}_p^H \mathbf{A}_p \mathbf{F}_p \right) \mathbf{x} - \left( \sum_p \mathbf{d}_p^H \mathbf{A}_p \mathbf{F}_p \right) \mathbf{x} \\
&\quad - \mathbf{x}^H \left( \sum_p \mathbf{F}_p^H \mathbf{A}_p^H \mathbf{d}_p \right) + \sum_p \mathbf{d}_p^H \mathbf{d}_p \\
&= \mathbf{x}^H \mathbf{P} \mathbf{x} - \mathbf{q}^H \mathbf{x} - \mathbf{x}^H \mathbf{q} + r
\end{aligned} \tag{3.12}$$

where  $\mathbf{P} = \sum_p \mathbf{F}_p^H \mathbf{A}_p^H \mathbf{A}_p \mathbf{F}_p$ ,  $\mathbf{q} = \sum_p \mathbf{F}_p^H \mathbf{A}_p^H \mathbf{d}_p$  and  $r = \sum_p \mathbf{d}_p^H \mathbf{d}_p$ . Problem  $P'$  is equivalent to the following problem:

$$(P) \begin{cases} \min_{\mathbf{x}} & \mathbf{x}^H \mathbf{P} \mathbf{x} - \mathbf{q}^H \mathbf{x} - \mathbf{x}^H \mathbf{q} + r \\ \text{s.t.} & |\mathbf{x}| = \mathbf{1} \end{cases} \tag{3.13}$$

which can be converted to the following problem with *real* (as opposed to complex) variables:

$$\begin{cases} \min_{\mathbf{u}} & \mathbf{u}^T \mathbf{G} \mathbf{u} - \mathbf{t}^T \mathbf{u} - \mathbf{u}^T \mathbf{t} + r \\ \text{s.t.} & u_l^2 + u_{l+L}^2 = 1, \quad l = 1, 2, \dots, L \end{cases} \tag{3.14}$$

where  $\mathbf{u} = [\text{Re}\{\mathbf{x}\}^T \text{Im}\{\mathbf{x}\}^T]^T$ ,  $u_l$  is the  $l$ -th element of  $\mathbf{u}$ ,  $L = MN$ ,

$$\mathbf{G} = \begin{bmatrix} \text{Re}\{\mathbf{P}\} & -\text{Im}\{\mathbf{P}\} \\ \text{Im}\{\mathbf{P}\} & \text{Re}\{\mathbf{P}\} \end{bmatrix} \text{ and } \mathbf{t} = \begin{bmatrix} \text{Re}\{\mathbf{q}\} \\ \text{Im}\{\mathbf{q}\} \end{bmatrix}$$

Problem (3.14) can be rewritten as:

$$(RP) \begin{cases} \min_{\mathbf{s}} & \mathbf{s}^T(\mathbf{R} + \lambda\mathbf{I})\mathbf{s} \\ \text{s.t.} & \mathbf{s}^T\mathbf{E}_l\mathbf{s} = 1, \quad l = 1, 2, \dots, L+1 \end{cases} \quad (3.15)$$

where  $\lambda$  is a positive number,

$$\mathbf{R} = \begin{bmatrix} \mathbf{G} & -\mathbf{t} \\ -\mathbf{t}^T & r \end{bmatrix}, \mathbf{s} = \begin{bmatrix} \mathbf{u} \\ 1 \end{bmatrix} = \begin{bmatrix} \text{Re}\{\mathbf{x}\} \\ \text{Im}\{\mathbf{x}\} \\ 1 \end{bmatrix},$$

and  $\mathbf{E}_l$  is a  $2L+1 \times 2L+1$  matrix given by:

$$\mathbf{E}_l(i, j) = \begin{cases} 1 & \text{if } i = j = l, \text{ and } l \leq L, \\ 1 & \text{if } i = l, j = l + L, \text{ and } l \leq L, \\ 1 & \text{if } i = j = 2L + 1, \text{ and } l = L + 1, \\ 0 & \text{Otherwise.} \end{cases}$$

Note that, since  $\sum_p \|\mathbf{d}_p - \mathbf{A}_p \mathbf{F}_p \mathbf{x}\|_2^2 = \mathbf{x}^H \mathbf{P} \mathbf{x} - \mathbf{q}^H \mathbf{x} - \mathbf{x}^H \mathbf{q} + r \geq 0$ , then, according to page 530 of [56],  $\mathbf{R}$  is positive semidefinite. Further, because the problem  $RP$  enforces  $\mathbf{s}^T \mathbf{E}_l \mathbf{s} = 1$ ,  $l = 1, 2, \dots, L$  then  $\lambda \mathbf{s}^T \mathbf{s}$  is a constant value (i.e.  $\lambda \mathbf{s}^T \mathbf{s} = \lambda(L+1)$ ). As a result, the optimal solution of  $P'$  and (the complex version of) the optimal solution of  $RP$  are identical for any  $\lambda \geq 0$ . Now, consider the following sequence of equality constrained QPs:

$$(CP^{(n)}) \begin{cases} \min_{\mathbf{s}} & \mathbf{s}^T(\mathbf{R} + \lambda\mathbf{I})\mathbf{s} \\ \text{s.t.} & \mathbf{B}^{(n)}\mathbf{s} = \mathbf{1} \end{cases} \quad (3.16)$$

where  $\mathbf{B}^{(n)} = [\mathbf{b}_1^{(n)}, \mathbf{b}_2^{(n)}, \dots, \mathbf{b}_{L+1}^{(n)}]^T \in \mathbb{R}^{(L+1) \times (2L+1)}$  such that the line defined by  $\mathbf{b}_l^{(n)T} \mathbf{s} = 1$  is a tangent to the circle  $\mathbf{s}^T \mathbf{E}_l \mathbf{s} = 1$  for  $l = 1, 2, \dots, L$  and  $\mathbf{b}_{L+1}^{(n)} = [0, \dots, 0, 1]^T$ . In particular, let  $\mathbf{s}^{(n)} \in \mathbb{R}^{(2L+1) \times 1}$  be the optimal solution of  $CP^{(n)}$  and  $\mathbf{x}^{(n)} \in \mathbb{C}^{L \times 1}$  be the complex version defined as:

$$x_l^{(n)} = s_l^{(n)} + j s_{l+L}^{(n)}, \quad l = 1, 2, \dots, L \quad (3.17)$$

where  $x_l^{(n)}$  and  $s_l^{(n)}$  are the  $l$ -th element of  $\mathbf{x}^{(n)}$  and  $\mathbf{s}^{(n)}$ , respectively. Thus,  $\mathbf{s}^{(n)} = [\text{Re}\{\mathbf{x}^{(n)}\}^T \text{Im}\{\mathbf{x}^{(n)}\}^T 1]^T$ . In this case, we define the matrix  $\mathbf{B}^{(n)}$  as:

$$\mathbf{B}^{(n)}(i, j) = \begin{cases} \cos(\arg x_l^{(n-1)}) & \text{if } i = j = l, \quad l \leq L, \\ \sin(\arg x_l^{(n-1)}) & \text{if } i = l, j = l + L, \quad l \leq L, \\ 1 & \text{if } i = L + 1, j = 2L + 1, \\ 0 & \text{Otherwise.} \end{cases}$$

Note that, problem  $CP^{(n)}$  is a convex quadratic minimization with linear equality constraints. Using the optimality conditions for problem  $CP^{(n)}$  [26], we have:

$$\overbrace{\begin{bmatrix} \bar{\mathbf{R}} & \mathbf{B}^{(n)T} \\ \mathbf{B}^{(n)} & \mathbf{0} \end{bmatrix}}^{\mathbf{K}} \begin{bmatrix} \mathbf{s}^{(n)} \\ \mathbf{v}^{(n)} \end{bmatrix} = \begin{bmatrix} \mathbf{0} \\ \mathbf{1} \end{bmatrix} \quad (3.18)$$

where  $\bar{\mathbf{R}} = 2(\mathbf{R} + \lambda\mathbf{I})$  and  $\mathbf{v}^{(n)} \in \mathbb{R}^{(L+1) \times 1}$  is the Lagrange multiplier associated with the equality constraints. Solving (3.18) by block elimination gives:

$$\mathbf{s}^{(n)} = \bar{\mathbf{R}}^{-1} \mathbf{B}^{(n)T} (\mathbf{B}^{(n)} \bar{\mathbf{R}}^{-1} \mathbf{B}^{(n)T})^{-1} \mathbf{1} \quad (3.19)$$

Since  $\mathbf{b}_1^{(n)}, \mathbf{b}_2^{(n)}, \dots, \mathbf{b}_{L+1}^{(n)}$  by construction are linearly independent for all  $n$  and  $\bar{\mathbf{R}}$  is positive definite for any  $\lambda > 0$ , then according to theorem 2.1 of [57] all the eigenvalues of  $\mathbf{K}$  in (3.18) are nonzero i.e.  $\mathbf{K}$  is nonsingular. As a consequence, equation (3.19) always has a unique solution  $\mathbf{s}^{(n)}$ .

Although the problem in (3.16) does not result in a constant modulus solution, a sequence of such problems (in the index  $n$ ) can ensure a non-increasing sequence of cost function values, such that the corresponding solution converges to constant modulus. To recognize this, let  $\mathbf{x}^{(n-1)}$  be the complex version defined in eq. (3.17), i.e.  $\mathbf{s}^{(n-1)} = [\text{Re}(\mathbf{x}^{(n-1)})^T \text{Im}(\mathbf{x}^{(n-1)})^T \mathbf{1}]^T$ . The affine constraints of  $CP^{(n)}$  are adjusted so that the feasible set of  $CP^{(n)}$  includes what we call as the *constant modulus version* of  $\mathbf{x}^{(n-1)}$  given by  $\mathbf{x}_{(n-1)} = \exp(j \arg(\mathbf{x}^{(n-1)}))$ . If  $\mathbf{x}^{(n)} = \mathbf{x}_{(n-1)}$ , then the constraints of the next problem  $CP^{(n+1)}$  are the same as problem  $CP^{(n)}$  which means  $\mathbf{x}^{(n+1)} = \mathbf{x}^{(n)}$  and, hence, the algorithm converges. Otherwise, the feasible set of  $CP^{(n)}$  is adapted to include the constant modulus version of  $\mathbf{x}^{(n-1)}$ . Convergence is then guaranteed by Lemma 3.3.1 which establishes that the cost function sequence that results by using the constant modulus version of the solution at each iteration, is in fact non-increasing and converges. This procedure is visually illustrated in Fig. 3.2.

The structure of this work bears a high level conceptual similarity to our recent work in SINR maximization [58] in that the solution in [58] also employs a sequence of convex problems approach. However, the cost function (minimization of deviation from an idealized beampattern vs. SINR maximization) as well as the actual sequence of problems (particularly the update of equality constraints in each iteration of the sequence) in this work are fundamentally different. Further, we establish new optimality properties of the solution (see Lemma 3.2) which was not considered in [58].

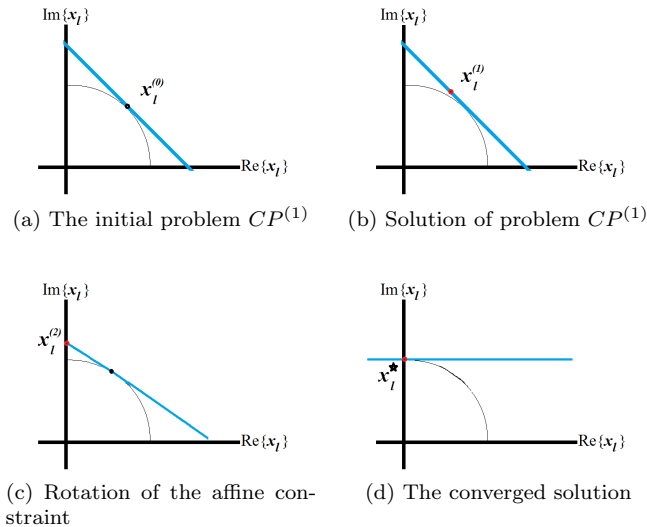


Figure 3.2: Illustration of the successive solutions of eq. (3.16).

### Convergence Analysis of SCF

The value of the objective function of problem ( $P$ ) as a function of the constant modulus version  $\mathbf{x}_{(n)}$  is non-increasing in  $n$ . This can be proved via the following Lemma.

**Lemma 3.3.1.** *Let  $\mathbf{x}^{(n)}$  be the complex version defined in (3.17). Denote by  $\mathbf{x}_{(n)}$  the constant modulus version of  $\mathbf{x}^{(n)}$ , i.e.  $\mathbf{x}_{(n)} = \exp(j \arg(\mathbf{x}^{(n)}))$ . Define  $f(\mathbf{x}) = \sum_p \|\mathbf{d}_p - \mathbf{A}_p \mathbf{F}_p \mathbf{x}\|_2^2$  and  $\lambda_{\mathbf{P}}$  as the maximum eigenvalue of  $\mathbf{P}$ . If  $\lambda \geq \frac{L}{8} \lambda_{\mathbf{P}} + \|\mathbf{q}\|_2$  then:*

$$f(\mathbf{x}_{(n-1)}) \geq f(\mathbf{x}_{(n)}) \quad (3.20)$$

*In other words, the sequence  $\{f(\mathbf{x}_{(n)})\}_{n=0}^{\infty}$  is non-increasing. Moreover, the sequence  $\{f(\mathbf{x}_{(n)})\}_{n=0}^{\infty}$  converges to a finite value  $f^*$ .*

It is well known in constrained optimization [26], that the first order necessary conditions for optimality are the so-called KarushKuhnTucker (KKT) conditions. So far, we have shown that our solution is feasible, i.e. a constant modulus is guaranteed at convergence. Now, we prove that the final converged solution of the proposed SCF algorithm is in fact KKT optimal.

**Lemma 3.3.2.** *Let  $C$  be the smallest number of iterations needed for convergence, i.e.  $f(\mathbf{x}_{(n-1)}) = f(\mathbf{x}_{(n)})$  for  $n \geq C$ . If  $\lambda \geq \frac{L}{8}\lambda_{\mathbf{P}} + \|\mathbf{q}\|_2$ , then for  $n \geq C$ :*

1.  $|\mathbf{x}^{(n)}| = \mathbf{1}$  .
2.  $\mathbf{x}^{(n)}$  is a KKT point of (P).

### Narrowband null forming beampattern design

Narrowband null forming beampattern design can be seen as a special case of our wideband beampattern design. In this case the beampattern design is conducted in spatial domain only i.e.  $N = 1$ . However, unlike the problem formulation in (3.8) the goal of null forming beampattern design is to form a beampattern with nulls in desired directions denoted by  $\{\theta_k\}_{k=1}^K$ . Let  $\mathbf{x} = [x_0 \ \dots \ x_{M-1}] \in \mathbb{C}^{M \times 1}$  where  $x_m$  is the coding waveform transmitted from the element  $m$ . The objective function can be defined as [53]:

$$f(\mathbf{x}) = \mathbf{x}^H \mathbf{V}^H \mathbf{\Sigma} \mathbf{V} \mathbf{x} \quad (3.21)$$

where  $\mathbf{V}$  and  $\mathbf{\Sigma}$  are expressed as:

$$\mathbf{V} = \begin{bmatrix} v_1(\theta_1) & v_1(\theta_2) & \dots & v_1(\theta_K) \\ v_2(\theta_1) & v_2(\theta_2) & \dots & v_2(\theta_K) \\ \vdots & \vdots & \ddots & \vdots \\ v_M(\theta_1) & v_M(\theta_2) & \dots & v_M(\theta_K) \end{bmatrix} \quad (3.22)$$

and,

$$\mathbf{\Sigma} = \text{diag}\{\sigma_1, \dots, \sigma_K\} \quad (3.23)$$

where  $v_m(\theta_k) = e^{j2\pi(f+f_c)\frac{m d \cos \theta_k}{c}}$  and  $\sigma_k$  is the weight factor of the radiation power in the  $k$ -th direction. Therefore, the problem can be formulated as:

$$\begin{cases} \min_{\mathbf{x}} & \mathbf{x}^H \mathbf{V}^H \mathbf{\Sigma} \mathbf{V} \mathbf{x} \\ \text{s.t.} & |\mathbf{x}| = \mathbf{1} \end{cases} \quad (3.24)$$

In this case, the optimization problem reduces to problem  $CP^{(n)}$  in (3.16) with:

$$\mathbf{R} = \begin{bmatrix} \text{Re}\{\mathbf{V}^H \mathbf{\Sigma} \mathbf{V}\} & -\text{Im}\{\mathbf{V}^H \mathbf{\Sigma} \mathbf{V}\} \\ \text{Im}\{\mathbf{V}^H \mathbf{\Sigma} \mathbf{V}\} & \text{Re}\{\mathbf{V}^H \mathbf{\Sigma} \mathbf{V}\} \end{bmatrix}, \mathbf{s} = \begin{bmatrix} \text{Re}\{\mathbf{x}\} \\ \text{Im}\{\mathbf{x}\} \end{bmatrix},$$

and  $\mathbf{B}^{(n)} = [\mathbf{b}_1^{(n)}, \mathbf{b}_2^{(n)}, \dots, \mathbf{b}_L^{(n)}]^T \in \mathbb{R}^{L \times 2L}$  given by:

$$\mathbf{B}^{(n)}(i, j) = \begin{cases} \cos(\arg x_i^{(n-1)}) & \text{if } i = j = l, \\ \sin(\arg x_i^{(n-1)}) & \text{if } i = l, j = l + L, \\ 0 & \text{Otherwise.} \end{cases}$$

Since  $\mathbf{V}^H \mathbf{\Sigma} \mathbf{V}$  is positive semi-definite and there are no linear terms in the objective function (i.e.  $\mathbf{q} = \mathbf{0}$ ), then both Lemma 3.3.1 and 3.3.2 hold for  $\lambda \geq \frac{L}{8}\lambda_{\mathbf{P}}$ .

## 3.4 Results and Discussions

### 3.4.1 Narrowband null forming beampattern

For narrowband beampattern design, the proposed method is compared to the state-of-the-art narrowband phase-only variable metric method (POVMM) method [39] and SDR with randomization [19].

- Experimental set up:** A linear MIMO radar antenna array of  $M = 16$  elements with half-wavelength spacing and  $\lambda = 0.1$ . Two beamforming cases are considered Case I:  $K = 1$ ,  $\theta_1 = -20^\circ$  and the wave factor  $\sigma_1 = 1$ ; Case II:  $K = 6$ ,  $\theta = [-60^\circ, -20^\circ, 20^\circ, 45^\circ, 60^\circ, 80^\circ]$  and the wave factors  $\sigma_k = 1/6$  for  $k = 1, 2, \dots, 6$ .
- Experimental Evaluation:** Figures 3.3 and ?? show the resulting beampattern for Case I and Case II, respectively. Clearly, SCF outperforms both SDR with randomization and POVMM by a significant amount. For example, in Fig. 3.3 at  $\theta_1 = -20^\circ$ , SCF has a null that is more than 100 dB lower than competing methods. The cost function defined by  $f(\mathbf{x}_{(n)}) = \mathbf{x}_{(n)}^H \mathbf{V}^H \mathbf{\Sigma} \mathbf{V} \mathbf{x}_{(n)}$  for the proposed SCF is non-increasing in each iteration as shown in Figure 3.6. Table 3.1 shows the cost function value as optimized via SCF as well as POVMM and their corresponding computational run times as observed in practice. Although POVMM has lower complexity per iteration, it needs orders of magnitude more iterations to achieve the same performance as SCF. Hence, for a given cost function (designed beam pattern deviation from idealized) specification, SCF can achieve it much sooner.

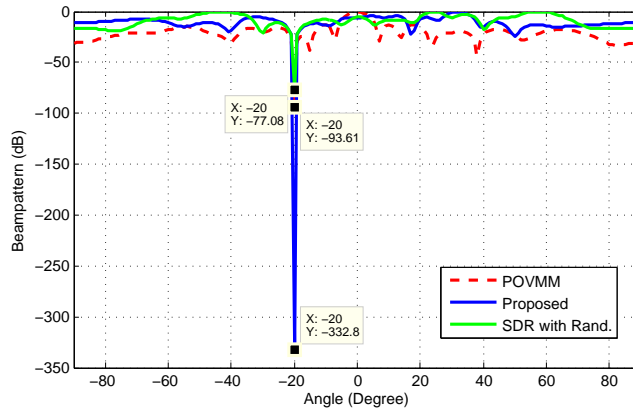


Figure 3.3: Beampattern of SDR with randomization[19], POVMM [39] and SCF for Case I.

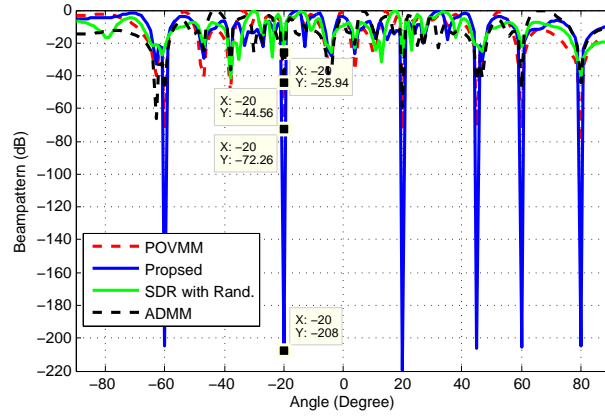


Figure 3.4: Beampattern of SDR with randomization[19], POVMM [39], ADMM [59] and SCF for Case III.

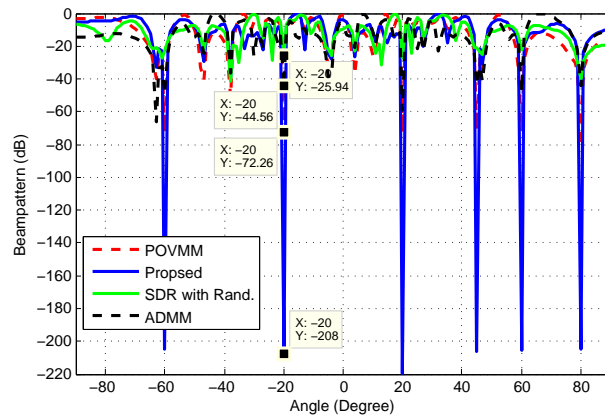


Figure 3.5: Beampattern of SDR with randomization[19], POVMM [39], ADMM [59] and SCF for Case III.

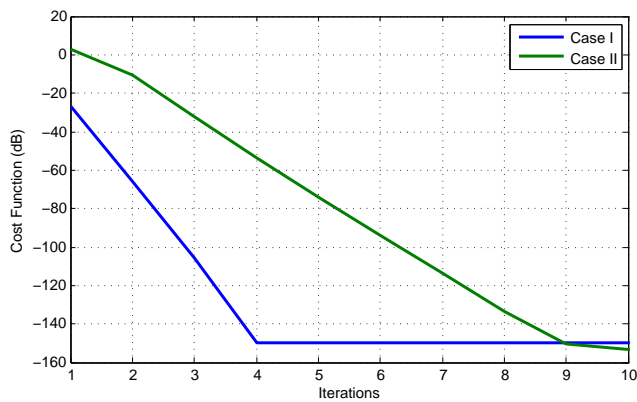


Figure 3.6: The cost function versus iterations of the proposed SCF method.

Table 3.1: Cost function in dB of SCF vs. POVMM, Case II

Method	Cost Function (dB)	Simu. Time (s)
POVMM (150 iterations)	-26.70	0.0122
POVMM (250 iterations)	-35.33	0.0178
POVMM (350 iterations)	-53.10	0.0240
SCF (9 iterations)	<b>-121.5</b>	<b>0.0117</b>

The effect of the number of antennas on the cost function is shown in Figure 3.7. In this case we used  $K = 2$ ,  $\theta = [-60^\circ, -63^\circ]$  and the wave factors  $\sigma_k = 1/2$  for  $k = 1, 2$ . Interestingly, the performance of the proposed SCF method with  $M = 6$  is comparable with the performance of POVMM with larger number of antennas  $M = 10$ .

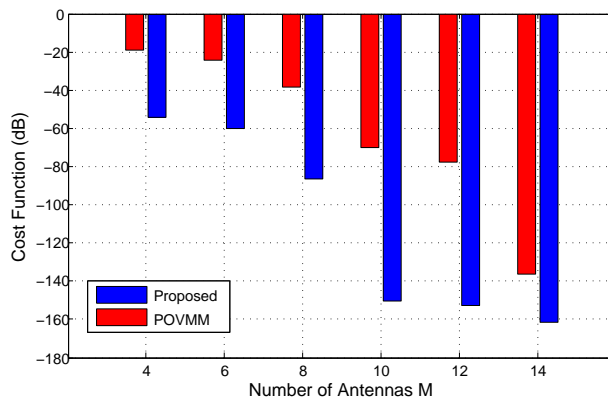


Figure 3.7: The cost function versus number of antennas for the proposed SCF method and POVMM[39].

Next, we consider the effect of random phase errors on the designed waveforms. The phase errors are incurred during waveform transmission and can be modeled as a random noise added to the designed waveform phase [53]. In the presence of phase errors hence, the actual transmitted waveforms are:

$$\tilde{\mathbf{x}} = [\exp(\arg(x_1) + e_1) \quad \dots \quad \exp(\arg(x_M) + e_M)]^T \quad (3.25)$$

where  $e_m$  is the random phase error for the waveform transmitted from the  $m$ -th antenna element. The random phase errors are modeled as statistically independent and Gaussian-distributed with zero mean and a standard deviation of  $\sigma_e$ .

Figure 3.8 shows a comparison between the ideal and the actual radiation beampattern of the SCF method with additive phase errors having a standard deviation of  $\sigma_e = 0.25$  for Case II. Fortunately, the average null depth of the actual radiation beampattern is about  $-61.34$  dB which is quite acceptable.

The average cost function over 1000 independent noise realizations of Case II ( $M = 16$ ) is listed in Table 3.2 for varying  $\sigma_e = 0.25$ . The SCF algorithm with 7 iterations outperforms the POVMM method for realistic values of  $\sigma_e$ .

Table 3.2: Effect of random phase errors on the performance (Cost Function in dB)

$\sigma_e$	0	0.1	0.25	0.5	1
POVMM	-35.33	-32.8	-31.11	-27.73	-22.77
SCF	-72.51	-43.2	-35.15	-29.23	-23.07

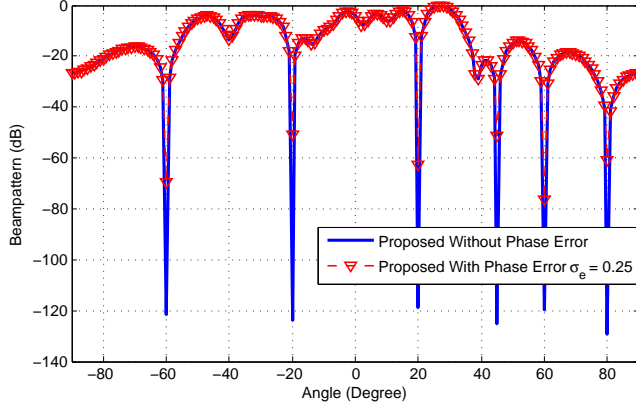


Figure 3.8: Effect of random phase error on the performance of SCF (Proposed) for Case II with phase deviation  $\sigma_e = 0.25$ .

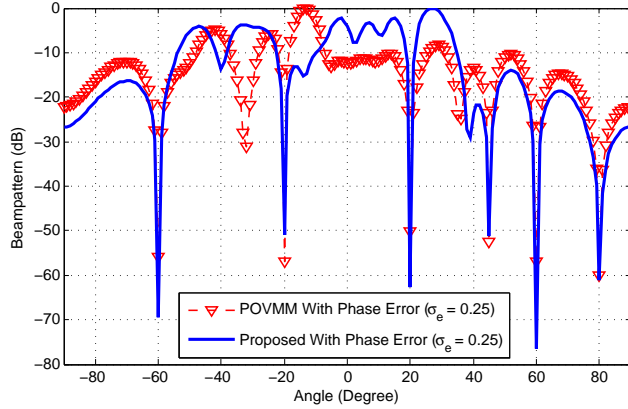


Figure 3.9: Effect of random phase error on the performance of POVMM and SCF (Proposed) for Case II with phase deviation  $\sigma_e = 0.25$ .

Figure 3.9 shows the actual radiation beampattern for waveform design for Case II with phase errors of standard deviation  $\sigma_e = 0.25$  of SCF compared to POVMM. The average null depth of the actual POVMM radiation beampattern is about  $-55.83$  dB which is about  $5.51$  dB higher than the average null depth of the actual SCF radiation beampattern.

### 3.4.2 Wideband beampattern

For wideband beampattern design, we compare SCF to the state-of-the-art Wideband Beampattern Formation via Iterative Techniques (WBFIT) method [51].

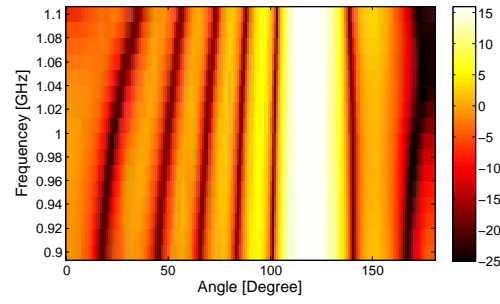
- **Experimental set up:** The following set-up is used in this numerical experiment: The number of transmit antennas  $M = 10$ , the number of time samples  $N = 32$ , the carrier frequency of the transmit signal  $f_c = 1$  GHz and the bandwidth  $B = 200$  MHz. The spatial angle is divided into  $K = 180$  grid points and we set  $\lambda = 10$ .

To provide an upper bound on achievable performance, we also obtain the beampattern as obtained by an unconstrained optimization of the transmit waveform, i.e. minimize (3.9) w.r.t  $\mathbf{x}$  but without any constraints on  $\mathbf{x}$ .

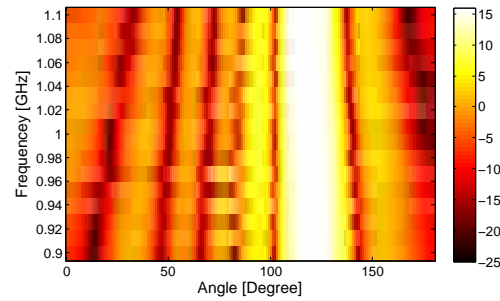
- **Experimental Evaluation:** *Example 1:* We consider the following desired transmit beampattern:

$$d(\theta, f) = \begin{cases} 1 & \theta = [120^\circ] \\ 0 & \text{Otherwise.} \end{cases}$$

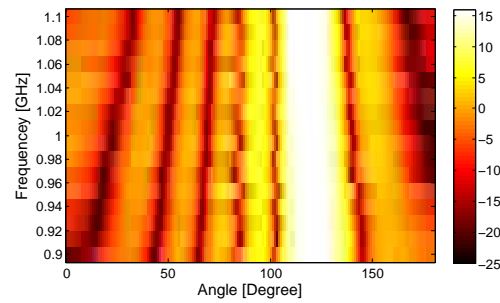
Fig. 3.10 shows the angle-frequency plot of the beampattern for (a) the unconstrained beampattern design (No CMC), (b) WBFIT method, (c) SDR with randomization and (d) SCF. In this somewhat favorable case, all three optimization methods produced a comparable radiation beampattern with SCF slightly outperforming WBFIT.



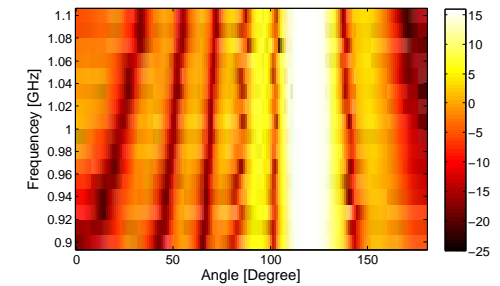
(a) Unconstrained



(b) WBFIT [51]



(c) SDR with rand. [19]



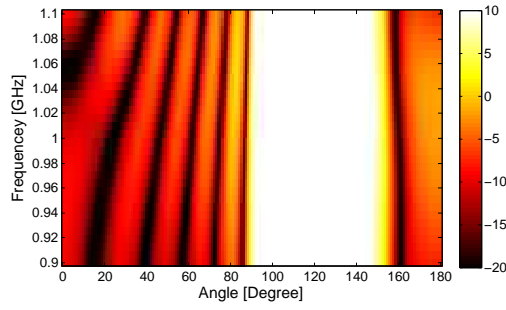
(d) SCF (Proposed)

Figure 3.10: Plot of the beampattern: (a) The unconstrained beampattern (b) WBFIT method (c) SDR with randomization (d) Proposed method

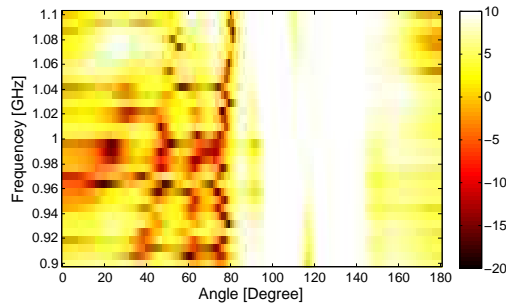
*Example 2:* We consider the following desired transmit beampattern:

$$d(\theta, f) = \begin{cases} 1 & \theta = [95^\circ, 145^\circ] \\ 0 & \text{Otherwise.} \end{cases}$$

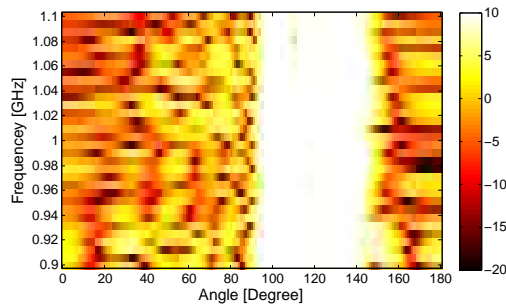
Fig. 3.11 shows the angle-frequency plot of the beampattern. Clearly, SCF is closer to the beampattern achieved by an unconstrained waveform and has higher suppression at the undesired angles compared to WBFIT and SDR with randomization with 10,000 randomization trials. Table 3.3 shows the the minimum cost function  $\sum_p \|\mathbf{d}_p - |\mathbf{A}_p \mathbf{F}_p \mathbf{x}^*|\|_2^2$  of the proposed method compared to WBFIT method and SDR with randomization. SCF achieves a cost function value that is 5.7 dB and 2 dB lower than WBFIT and SDR with randomization, respectively, which indicates that the proposed method is much closer to the desired beampattern.



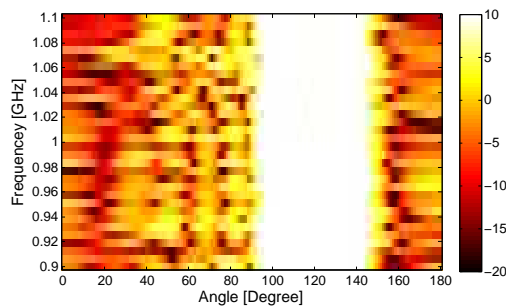
(a) Unconstrained



(b) WBFIT [51]



(c) SDR with rand. [19]



(d) SCF (Proposed)

Figure 3.11: Plot of the beam pattern: (a) The unconstrained beam pattern (b) WBFIT method (c) SDR with randomization (d) Proposed method

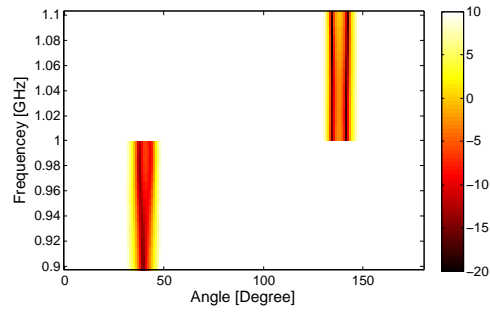
*Example 3:* We consider another example where we have different beam pattern shape in different frequency bands. In particular, we consider the following desired beam pattern:

Table 3.3: Cost function in dB of the proposed method vs. WBFIT (Case I)

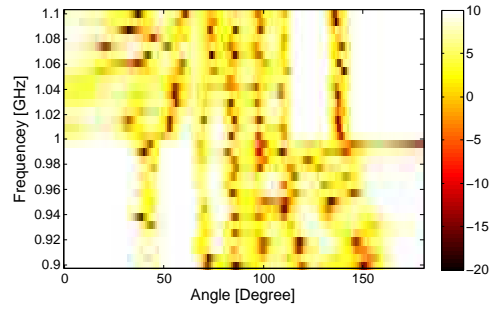
Method	Cost Function (dB)
Unconstrained	19.93
WBFIT[51]	29.24
SDR with rand.[19]	25.5
SCF	<b>23.54</b>

$$d(\theta, f) = \begin{cases} 1 & \theta = [30^\circ, 50^\circ], -B/2 + f_c \leq f \leq f_c \\ 1 & \theta = [130^\circ, 150^\circ], f_c < f \leq B/2 + f_c \\ 0 & \text{Otherwise.} \end{cases}$$

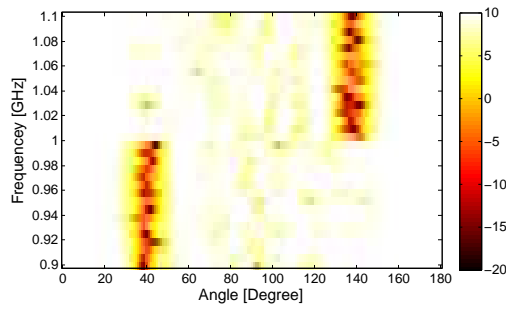
Fig. 3.12 shows the angle-frequency plot of the beampattern. Clearly, SCF is closer to the beampattern achieved by an unconstrained waveform and has higher suppression at the undesired angles compared to WBFIT. Table 3.4 shows the the minimum cost function  $\sum_p \|\mathbf{d}_p - |\mathbf{A}_p \mathbf{F}_p \mathbf{x}^*\|_2^2$  of the proposed method compared to WBFIT method. In this case, the difference between SCF and both WBFIT and SDR with randomization is higher, as SCF achieves a cost function value that is 7.5 dB and 5 dB lower than WBFIT and SDR with randomization, respectively.



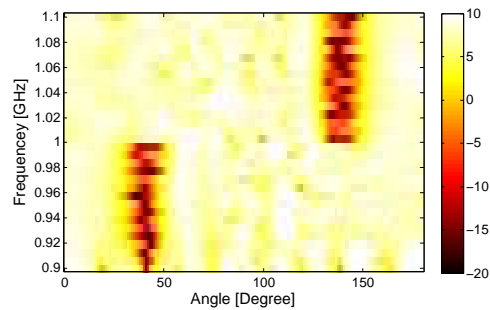
(a) Unconstrained



(b) WBFIT [51]



(c) SDR with rand. [19]



(d) SCF (Proposed)

Figure 3.12: Plot of the beampattern: (a) The unconstrained beampattern (b) WBFIT method (c) SDR with randomization (d) Proposed method

Table 3.4: Cost function in dB of the proposed method vs. WBFIT (Case II)

<b>Method</b>	<b>Cost Function (dB)</b>
Unconstrained	19.38
WBFIT[51]	32.38
SDR with rand.[19]	29.2
SCF	<b>24.1</b>

### 3.5 Conclusions

Our work achieves tractable beampattern design by waveform synthesis for MIMO radar in the presence of constant modulus. The central idea of our analytical contribution is to successively achieve constant modulus (at convergence), while solving an equality constrained quadratic program in each step of the sequence. Because each such problem in the sequence has a closed form (SCF), this makes our method computationally attractive. We establish new analytical properties of the SCF algorithm as well as the converged solution. Further, we show experimentally that the proposed SCF can achieve superior beampattern accuracy compared to state-of-the-art. Future work could consider the incorporation of more constraints on the beampattern design, such as a waveform similarity [16, 60] and/or a spectral interference constraint.

## Chapter 4

# Spatio-Spectral Radar Beampattern Design for Co-existence with Wireless Communication Systems

### 4.1 Summary

Co-existence of radar and telecommunication systems has been an emerging requirement recently [61, 62, 63, 64, 65, 66, 67, 68, 69]. A priori knowledge about expected target locations and the radio frequency environment enables MIMO radar systems to enhance the probability of detection while ensuring compatibility with civilian wireless systems. Specifically, the MIMO radar should focus the radiation beam in the expected target directions while maintaining a low spectral interference level at specific bands used by other licensed wireless systems. These two objectives can be achieved by constrained optimization of the radar transmit waveform [70, 71].

Two main research directions of radar beampattern/waveform optimization have been actively pursued to ensure co-existence of radar and communication systems in the past years. First, optimization of MIMO radar waveform to match the desired beampattern with an arbitrary spectrum shape has been a topic of much recent interest [72, 73, 74, 75, 76, 77, 78, 79, 80, 81, 82, 83, 84, 85, 86]. In these methods, the goal of the optimization problem is to minimize deviation of the optimized beampattern to the desired one which is designed to reduce the transmit energy at *spatial* angles where the communication systems are located. Some of these works focus on receive beampattern design [79, 85, 86] while most others focus on the transmit beampattern design. On the other hand, mitigation of the energy of the transmit waveform in the *spectral* frequency bands occupied by wireless communication systems has also been studied [87]. This approach matches the spectral shape of the optimized waveform to the desired one which is designed to limit the interference level on communication systems or to directly minimize the interference level at communication receivers. However, since the beampattern is not considered, it is not able to control the radiation beam in spatial directions.

#### 4.1.1 Motivation and Challenges

In practice, the transmit beampattern design is more challenging for two reasons. The first reason is the requirement of the constant modulus constraint on the radar transmit waveform, i.e. a constant envelope transmit signal [88]. The importance of the constant modulus waveform has been well documented and analyzed in terms of performance loss [88, 89, 90]. A non-linear power amplifier which is equipped in most radar systems cannot be efficiently utilized without the constant modulus constraint since the output of the amplifier will be a clipped version of the optimized waveform. The second reason is the requirement of spectral compatibility of radar and telecommunication systems, which demands a spectral constraint on the radar waveform spectral shape. Designing the MIMO radar beampattern in the simultaneous presence of constant modulus and spectral constraints remains a stiff

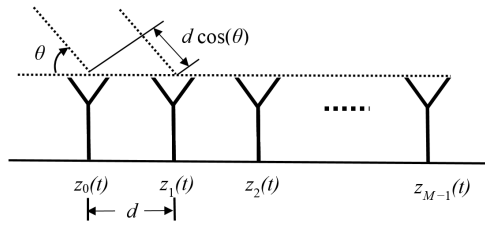


Figure 4.1: Configuration of ULA antenna

open challenge.

It is well known that the MIMO transmit beampattern/waveform design subject to the constant modulus constraint constitutes a hard non-convex problem. To ensure tractability, some existing approaches pursue relaxations to energy constraint (using  $L2$  norm) [61, 91] or approximations to the constant modulus constraint [80, 83, 87]. This indirect approximation makes the problem more tractable, however, it degrades the design accuracy. Some recent efforts directly enforce the constant modulus constraint and hence lead to better performance. However, they invariably involve semi-definite relaxation (SDR) with randomization [92, 93]. In this approach, a semi-definite programming (SDP) is first solved to find a waveform distribution. Then a large number of random waveforms are generated based on this distribution, which is followed by an exhaustive search to find the closest waveform. Despite the success of SDR for constant modulus constrained problems, two issues remain: 1.) extensions to spectral constraints, which are quadratic inequalities are *not* straightforward, and 2.) the computational burden is high.

Beampattern design under the constant modulus constraint but without the spectral constraint has been studied in [72, 74, 73, 83, 94, 84]. In the beampattern design problems, an approximation to constant modulus was pursued using the peak-to-average power ratio (PAPR) waveform constraint [80, 83]. While the constant modulus constraint is not explicitly represented in the optimization process, the resulting solution is converted to the nearest constant modulus solution.

## 4.2 Introduction

### 4.2.1 System Model

Consider a wideband MIMO radar with a uniform linear array (ULA) of  $M$  antennas and equal spacing distance of  $d$  as shown in Fig. 4.1. The signal transmitted from the  $m$ -th element is denoted by  $z_m(t)$ . Let  $z_m(t) = x_m(t)e^{j2\pi f_c t}$  where  $x_m(t)$  is the baseband signal and  $f_c$  is the carrier frequency. We assume that the spectral support of  $x_m(t)$  is within the interval  $[-B/2, B/2]$  where  $B$  is the bandwidth in Hz. The sampled baseband signal transmitted by the  $m$ -th element is denoted by  $x_m(n) \triangleq x_m(t = nT_s)$ ,  $n = 0, \dots, N - 1$  with  $N$  being the number of time samples and  $T_s = 1/B$  is the sampling rate. The discrete Fourier transform (DFT) of  $x_m(n)$  is denoted by  $y_m(p)$  and it is given by

$$y_m(p) = \sum_{n=0}^{N-1} x_m(n) e^{-j2\pi \frac{np}{N}}, \quad p = -\frac{N}{2}, \dots, 0, \dots, \frac{N}{2} - 1 \quad (4.1)$$

### 4.2.2 Far-Field Beampattern

According to [83], the discrete frequency beampattern at the angle  $\theta$  in the frequency band  $p$  in the far-field is given by

$$P(\theta, p) = |\mathbf{a}^H(\theta, p) \mathbf{y}_p|^2 \quad (4.2)$$

where

$$\mathbf{a}(\theta, p) = [1 \quad e^{j2\pi(\frac{p}{NT_s} + f_c) \frac{d \cos \theta}{c}} \quad \dots \quad e^{j2\pi(\frac{p}{NT_s} + f_c) \frac{(M-1)d \cos \theta}{c}}]^T \quad (4.3)$$

and

$$\mathbf{y}_p = [y_0(p) \quad y_1(p) \quad \dots \quad y_{M-1}(p)]^T \quad (4.4)$$

where  $c$  is the speed of wave propagation. Note that  $\mathbf{a}(\theta, p)$  is continuous in phase. It can be expressed as a discrete angle vector by dividing the interval  $[0^\circ, 180^\circ]$  into  $K$  angle bins. Using the same simplified notation found in [83], it can be written as

$$\mathbf{a}_{kp} = \mathbf{a}(\theta_k, p), \quad k = 1, 2, \dots, K \quad (4.5)$$

In this case, the beampattern can be given by the following discrete angle-frequency grid

$$P_{kp} = |\mathbf{a}_{kp}^H \mathbf{y}_p|^2 = |\mathbf{a}_{kp}^H \mathbf{W}_p \mathbf{x}|^2 \quad (4.6)$$

where  $\mathbf{x} \in \mathbb{C}^{MN}$  is the concatenated vector i.e.  $\mathbf{x} = [\mathbf{x}_0^T \quad \mathbf{x}_1^T \quad \dots \quad \mathbf{x}_{M-1}^T]^T$  where  $\mathbf{x}_m = [x_m(0) \quad x_m(1) \quad \dots \quad x_m(N-1)]^T \in \mathbb{C}^N$  and  $\mathbf{W}_p \in \mathbb{C}^{M \times MN}$  is given by

$$\mathbf{W}_p = \mathbf{I}_M \otimes \mathbf{e}_p^H \quad (4.7)$$

where  $\otimes$  is a Kronecker product operator,  $\mathbf{e}_p^H = [1 \quad e^{-j2\pi \frac{p}{N}} \quad \dots \quad e^{-j2\pi \frac{(N-1)p}{N}}] \in \mathbb{C}^N$  and  $\mathbf{I}_M$  is an  $M \times M$  identity matrix.

### 4.2.3 Formulation of the Spectral Constraint

The problem of spectral co-existence has been of great interest recently [61, 62, 63, 64, 65, 66, 67, 68, 69] and involves minimization of interference caused by radar transmission at victim communication receivers operating in the same frequency band. In this case, the beampattern of the transmit waveform is required to have nulls in these bands to prevent interference. For  $J$  communication receivers, we suppose that the  $j$ -th communication receiver operating on a frequency band  $B_j = [p_l^j, p_u^j]$ , where  $p_l^j$  and  $p_u^j$  are the lower and upper normalized frequency, respectively. We denote the desired (discrete) spectrum shape by  $\hat{\mathbf{y}} = [\hat{y}_{-\frac{N}{2}}, \hat{y}_{-\frac{N}{2}+1}, \dots, \hat{y}_{\frac{N}{2}-1}] \in \mathbb{C}^{N \times 1}$  defined as

$$\hat{y}_p = \begin{cases} 0 & \text{for } p \in B_j = [p_l^j, p_u^j], \quad j = 1, 2, \dots, J \\ \gamma & \text{otherwise.} \end{cases}$$

where  $\gamma$  is a scalar such that  $\hat{\mathbf{y}}^H \mathbf{F} \mathbf{F}^H \hat{\mathbf{y}} = N$  and  $\mathbf{F}$  is the DFT matrix. In SHAPE algorithm proposed by Rowe *et al.* [87], a least-squares fitting approach for the spectral shaping problem for SISO has been formulated by minimizing the following cost function

$$\|\mathbf{F}^H \mathbf{x} - \hat{\mathbf{y}}\|_2^2 \quad (4.8)$$

where the phase vector  $\beta$  is an auxiliary vector and  $\odot$  represents the element-wise product operation. We extend (4.8) for MIMO radar and employ it as a constraint in the optimization problem as follows

$$\|(\mathbf{I}_M \otimes \mathbf{F}^H)(\mathbf{1}_M \otimes \hat{\mathbf{y}}) - \mathbf{x}\|_2^2 = \|\bar{\mathbf{F}}^H \bar{\mathbf{y}} - \mathbf{x}\|_2^2 \leq E_R \quad (4.9)$$

where  $\mathbf{1}_M = [1, 1, \dots, 1] \in \mathbb{R}^{M \times 1}$ ,  $\bar{\mathbf{F}} = \mathbf{I}_M \otimes \mathbf{F}^H$ , and  $\bar{\mathbf{y}} = \mathbf{1}_M \otimes \hat{\mathbf{y}}$ , and  $E_R$  is the maximum tolerable spectral error.

### 4.2.4 Problem Formulation

The optimization problem can be formulated as the following matching problem:

$$\begin{cases} \min_{\mathbf{x}} & \sum_{k=1}^K \sum_{p=-\frac{N}{2}}^{\frac{N}{2}-1} [d_{kp} - |\mathbf{a}_{kp}^H \mathbf{W}_p \mathbf{x}|]^2 \\ \text{s.t.} & |\mathbf{x}| = \mathbf{1} \\ & \|\bar{\mathbf{F}}^H \bar{\mathbf{y}} - \mathbf{x}\|_2^2 \leq E_R \end{cases} \quad (4.10)$$

where  $d_{kp} \in \mathbb{R}$  is the desired beampattern. The constant modulus constraints ( $|\mathbf{x}| = \mathbf{1}$ ) implies that  $|x_m(n)| = 1$  for  $m = 1, \dots, M$  and  $n = 0, \dots, N-1$ . These constraints are neither convex nor linear and it is well known in the literature that (4.10) is a hard non-convex problem even without the spectral constraint. He *et al.* [83] proposed a solution to problem (4.10) without the spectral

constraint by employing a peak-to-average ratio constraint as a relaxation of the constant modulus constraint. However, they used the cyclic algorithm [95, 96] to solve the unconstrained problem  $\min_{\mathbf{y}_p} \sum_{k=1}^K \sum_{p=-\frac{N}{2}}^{\frac{N}{2}-1} [d_{kp} - |\mathbf{a}_{kp}^H \mathbf{y}_p|]^2$  in the first stage and then in the second stage they aim to find the constant modulus approximation of the solution. The algorithm does not directly minimize the cost function under constant modulus constraint or any relaxed version thereof. In this paper, we propose a new solution that minimizes the cost function of interest subject to the constant modulus constraint and the spectral constraint by solving a sequence of problems under a relaxed convex constraint such that constant modulus is still achieved at convergence. The proposed new solution has the ability to break the computational cost-solution quality trade-off that has been demonstrated in past work such as SDR with randomization [93, 92] or the simulated annealing approach [83].

*Remark:* The cost function of (4.10) can be modified as follows:  $\sum_{k=1}^K \sum_{p=-\frac{N}{2}}^{\frac{N}{2}-1} w_{kp} [d_{kp} - |\mathbf{a}_{kp}^H \mathbf{W}_p \mathbf{x}|]^2$  to control the relative importance of certain frequency bands or angles; where  $w_{kp}$  are positive weights such that  $\sum_{k=1}^K \sum_{p=-\frac{N}{2}}^{\frac{N}{2}-1} w_{kp} = 1$ . Note such a modification can also be easily accommodated in the analytical development presented next.

## 4.3 Methods, Assumptions, and Procedures

### 4.3.1 Overview of Contribution

Our principal aim is to develop an algorithmic approach for *spatio-spectral* MIMO beampattern design. Closeness to an idealized beampattern that minimizes radar energy in the direction of wireless communication receivers captures the spatial component while the spectral component of our approach involves explicitly forcing a spectral fidelity constraint.

Specifically, this paper makes the following contributions:

- **A new algorithmic solution for spatio-spectral beampattern design under both the spectral constraint and the constant modulus constraint.** To overcome the challenges mentioned above, we develop a new algorithm for MIMO beampattern design that involves solving the hard non-convex problem of beampattern design using a sequence of convex equality and inequality constrained quadratic programs (QP), each of which has a closed form solution, such that constant modulus is achieved at convergence. Because each QP in the sequence has a closed form solution, the proposed beampattern with interference control (BIC) algorithm has significantly lower complexity than most competing methods.
- **Feasibility of the sequence of QPs.** Assuming that the original non-convex problem of beampattern design is feasible, i.e. the intersection set of constant modulus and spectral constraints is non-empty; we formally prove that each QP we formulate in the aforementioned BIC sequence is also guaranteed to be feasible.
- **Convergence of the BIC algorithm.** We establish that the sequence of cost functions representing a deviation from the desired beampattern, that occurs in the proposed BIC algorithm, is non-increasing, (i.e. an improvement is always obtained by solving each problem in the sequence) and converges.
- **Experimental insights and validation.** Experimental validation is performed across two scenarios: 1) null forming where the BIC algorithm shows significant power suppression in the desired directions even in the presence of the spectral constraint, and 2) full beampattern design where the proposed BIC is shown to achieve a beampattern much closer to the ground truth against state of the art alternatives that have no spectral interference constraint.

## 4.4 Beampattern Design under Constant Modulus and Spectral Constraints

### 4.4.1 Non-convex Optimization Problem

As shown in [83], it is more convenient to rewrite the objective function of (4.10) as

$$\sum_{k=1}^K \sum_{p=-\frac{N}{2}}^{\frac{N}{2}-1} |d_{kp} e^{j\phi_{kp}} - \mathbf{a}_{kp}^H \mathbf{W}_p \mathbf{x}|^2 \quad (4.11)$$

where  $\phi_{kp} = \arg\{\mathbf{a}_{kp}^H \mathbf{W}_p \mathbf{x}\}$ . Since  $\mathbf{x}$  is unknown,  $\phi_{kp}$  is also unknown for all  $k$  and  $p$ . In the existing literature [83, 95, 96], this problem has been resolved by an iterative method. This method first minimizes Eq. (4.11) w.r.t.  $\mathbf{x}$  for a fixed values of  $\{\phi_{kp}\}$  and then finds the optimal  $\{\phi_{kp}\}$  for the fixed  $\mathbf{x}$  obtained in the previous iteration step. It has been shown that such an iterative method ensures that the cost function is monotonically decreasing and converges to a finite value. Therefore, we focus on solving the following constrained problem for a fixed  $\{\phi_{kp}\}$ .

$$\begin{cases} \min_{\mathbf{x}} & \sum_{k=1}^K \sum_{p=-\frac{N}{2}}^{\frac{N}{2}-1} |d_{kp} e^{j\phi_{kp}} - \mathbf{a}_{kp}^H \mathbf{W}_p \mathbf{x}|^2 \\ \text{s.t.} & |\mathbf{x}| = 1 \\ & \|\bar{\mathbf{F}}^H \bar{\mathbf{y}} - \mathbf{x}\|_2^2 \leq E_R \end{cases} \quad (4.12)$$

First, let us define the following

$$\mathbf{A}_p = \begin{bmatrix} \mathbf{a}_{1p}^H \\ \vdots \\ \mathbf{a}_{Kp}^H \end{bmatrix}, \quad \mathbf{d}_p = \begin{bmatrix} d_{1p} e^{j\phi_{1p}} \\ \vdots \\ d_{Kp} e^{j\phi_{Kp}} \end{bmatrix} \quad (4.13)$$

Then the objective function of (4.12) can be rewritten in terms of  $\mathbf{A}_p$  and  $\mathbf{d}_p$  [84]

$$f(\mathbf{x}) = \sum_p \|\mathbf{d}_p - \mathbf{A}_p \mathbf{W}_p \mathbf{x}\|_2^2 \quad (4.14)$$

$$= \mathbf{x}^H \mathbf{P} \mathbf{x} - \mathbf{q}^H \mathbf{x} - \mathbf{x}^H \mathbf{q} + r \quad (4.15)$$

where  $\mathbf{P} = \sum_p \mathbf{W}_p^H \mathbf{A}_p^H \mathbf{A}_p \mathbf{W}_p$ ,  $\mathbf{q} = \sum_p \mathbf{W}_p^H \mathbf{A}_p^H \mathbf{d}_p$  and  $r = \sum_p \mathbf{d}_p^H \mathbf{d}_p$ . Moreover, the spectral constraint can also be simplified as

$$\begin{aligned} \|\bar{\mathbf{F}}^H \bar{\mathbf{y}} - \mathbf{x}\|_2^2 &= (\bar{\mathbf{F}}^H \bar{\mathbf{y}} - \mathbf{x})^H (\bar{\mathbf{F}}^H \bar{\mathbf{y}} - \mathbf{x}) \\ &= \mathbf{x}^H \mathbf{x} - 2 \operatorname{Re}\{\bar{\mathbf{y}}^H \bar{\mathbf{F}} \mathbf{x}\} + \bar{\mathbf{y}}^H \bar{\mathbf{F}} \bar{\mathbf{F}}^H \bar{\mathbf{y}} \\ &= 2L - 2 \operatorname{Re}\{\bar{\mathbf{y}}^H \bar{\mathbf{F}} \mathbf{x}\} \end{aligned}$$

where  $L = MN$ . Hence, the spectral constraint can be rewritten as

$$\operatorname{Re}\{\bar{\mathbf{y}}^H \bar{\mathbf{F}} \mathbf{x}\} \geq (1 - E_R/2)L$$

The optimization problem (4.12) is equivalent to the following problem.

$$\begin{cases} \min_{\mathbf{x}} & \mathbf{x}^H \mathbf{P} \mathbf{x} - \mathbf{q}^H \mathbf{x} - \mathbf{x}^H \mathbf{q} + r \\ \text{s.t.} & |\mathbf{x}| = 1 \\ & \operatorname{Re}\{\bar{\mathbf{y}}^H \bar{\mathbf{F}} \mathbf{x}\} \geq (1 - E_R/2)L \end{cases} \quad (4.16)$$

Moreover,  $f(\mathbf{x})$  can be converted to the following function with *real* (as opposed to complex) variables.

$$f_R(\mathbf{u}) = \mathbf{u}^T \mathbf{G} \mathbf{u} - \mathbf{t}^T \mathbf{u} - \mathbf{u}^T \mathbf{t} + r \quad (4.17)$$

where

$$\mathbf{u} = [\operatorname{Re}\{\mathbf{x}\}^T \operatorname{Im}\{\mathbf{x}\}^T]^T \quad (4.18)$$

$$\mathbf{G} = \begin{bmatrix} \operatorname{Re}\{\mathbf{P}\} & -\operatorname{Im}\{\mathbf{P}\} \\ \operatorname{Im}\{\mathbf{P}\} & \operatorname{Re}\{\mathbf{P}\} \end{bmatrix} \quad (4.19)$$

$$\mathbf{t} = \begin{bmatrix} \operatorname{Re}\{\mathbf{q}\} \\ \operatorname{Im}\{\mathbf{q}\} \end{bmatrix} \quad (4.20)$$

The problem (4.16) can be rewritten as

$$\begin{cases} \min_{\mathbf{s}} & \mathbf{s}^T (\mathbf{R} + \lambda \mathbf{I}) \mathbf{s} \\ \text{s.t.} & \mathbf{s}^T \mathbf{E}_l \mathbf{s} = 1, \quad l = 1, 2, \dots, L \\ & \bar{\mathbf{s}}^T \mathbf{s} \geq (1 - E_R/2)L \end{cases} \quad (4.21)$$

where  $\lambda$  is an arbitrary positive number,

$$\bar{\mathbf{s}} = [\operatorname{Re}\{\bar{\mathbf{F}}^H \bar{\mathbf{y}}\}^T \operatorname{Im}\{\bar{\mathbf{F}}^H \bar{\mathbf{y}}\}^T 0]^T, \quad (4.22)$$

$$\mathbf{R} = \begin{bmatrix} \mathbf{G} & -\mathbf{t} \\ -\mathbf{t}^T & r \end{bmatrix}, \quad (4.23)$$

$$\mathbf{s} = \begin{bmatrix} \operatorname{Re}\{\mathbf{x}\} \\ \operatorname{Im}\{\mathbf{x}\} \\ 1 \end{bmatrix}, \quad (4.24)$$

and  $\mathbf{E}_l$  is a  $2L + 1 \times 2L + 1$  matrix given by

$$\mathbf{E}_l(i, j) = \begin{cases} 1 & \text{if } i = j = l \\ 1 & \text{if } i = l + L, j = l + L \\ 0 & \text{otherwise.} \end{cases} \quad (4.25)$$

Note that, since

$$\mathbf{s}^T \mathbf{R} \mathbf{s} = \mathbf{x}^H \mathbf{P} \mathbf{x} - \mathbf{q}^H \mathbf{x} - \mathbf{x}^H \mathbf{q} + r \quad (4.26)$$

$$= \sum_p \|\mathbf{d}_p - \mathbf{A}_p \mathbf{W}_p \mathbf{x}\|_2^2 \quad (4.27)$$

$$\geq 0 \quad (4.28)$$

,  $\mathbf{R}$  is positive semi-definite. Further, because the problem (4.21) enforces constant modulus, i.e.,  $\mathbf{s}^T \mathbf{E}_l \mathbf{s} = 1$  for  $l = 1, 2, \dots, L$ ,  $\lambda \mathbf{s}^T \mathbf{s}$  is a constant value ( $\lambda \mathbf{s}^T \mathbf{s} = \lambda(L + 1)$ ). As a result, (4.10) and (4.21) are the identical optimization problems and the optimal solution of (4.10) and (the complex version of) the optimal solution of (4.21) are also identical for any  $\lambda \geq 0$ .

#### 4.4.2 Sequence of Closed Form Solutions

Now we focus on solving (4.21). Though it is minimization of a convex objective function, it is still non-convex because of the constant modulus constraint. We propose a new sequential approach to solve (4.21) which involves solving a sequence of convex problems. Let us consider the following sequence of constrained QPs where the  $n$ -th QP is given by

$$(CP)^{(n)} \begin{cases} \min_{\mathbf{s}} & \mathbf{s}^T (\mathbf{R} + \lambda \mathbf{I}) \mathbf{s} \\ \text{s.t.} & \mathbf{B}^{(n)} \mathbf{s} = \mathbf{1} \\ & \bar{\mathbf{s}}^{(n)T} \mathbf{s} \geq (1 - E_R/2)L \end{cases} \quad (4.29)$$

where  $\bar{\mathbf{s}}^{(n)}$  is given by:

$$\bar{\mathbf{s}}^{(n)} = \begin{bmatrix} \text{Re}\{(\bar{\mathbf{F}}^H \bar{\mathbf{y}}) \odot e^{j \arg(\mathbf{x}^{(n-1)}) - \arg(\bar{\mathbf{F}}^H \bar{\mathbf{y}})}\} \\ \text{Im}\{(\bar{\mathbf{F}}^H \bar{\mathbf{y}}) \odot e^{j \arg(\mathbf{x}^{(n-1)}) - \arg(\bar{\mathbf{F}}^H \bar{\mathbf{y}})}\} \\ 0 \end{bmatrix} \quad (4.30)$$

and  $\mathbf{B}^{(n)} = [\mathbf{b}_1^{(n)}, \mathbf{b}_2^{(n)}, \dots, \mathbf{b}_{L+1}^{(n)}]^T \in \mathbb{R}^{(L+1) \times (2L+1)}$  such that the line defined by  $\mathbf{b}_l^{(n)T} \mathbf{s} = 1$  is a tangent to the circle  $\mathbf{s}^T \mathbf{E}_l \mathbf{s} = 1$  for  $l = 1, 2, \dots, L$ . Specifically,  $\mathbf{b}_l$  is given by

$$\mathbf{b}_l^{(n)}(i) = \begin{cases} \cos(\gamma_l^{(n)}) & \text{if } i = l \\ \sin(\gamma_l^{(n)}) & \text{if } i = l + L \\ 0 & \text{otherwise.} \end{cases} \quad (4.31)$$

for  $l = 1, \dots, L$  and  $\mathbf{b}_{L+1}^{(n)} = [0, \dots, 0, 1]^T$  where  $\gamma_l^{(n)} = 2 \arg(x_l^{(n-1)}) - \gamma_l^{(n-1)}$  and  $x_l^{(n)}$  is the  $l$ -th elements of  $\mathbf{x}^{(n)}$  which is the complex version of the optimal solution of (4.29),  $\mathbf{s}^{(n)}$ , that is,  $x_l^{(n)} = s_l^{(n)} + j s_{l+L}^{(n)}$  and conversely  $\mathbf{s}^{(n)} = [\text{Re}\{\mathbf{x}^{(n)}\}^T \text{Im}\{\mathbf{x}^{(n)}\}^T \mathbf{1}]^T$ .

Although the problem (4.29) does not result in a constant modulus solution, a sequence of such problems (in the index  $n$ ) ensures a non-increasing sequence of cost function values, such that the sequence of the corresponding optimal solutions converges to constant modulus for large enough  $\lambda^1$ . To recognize this, we first show that the constraints of  $CP^{(n)}$  in (4.29) are adjusted so that the feasible set of  $CP^{(n)}$  includes  $\mathbf{x}^{(n-1)}$ .

**Lemma 4.4.1.** *The feasible set of problem  $CP^{(n)}$  contains the optimal solution of problem  $CP^{(n-1)}$ .*

*Proof.* Let  $\mathbf{s}^{(n-1)}$  be the optimal solution of  $CP^{(n-1)}$ . Then  $\mathbf{B}^{(n-1)} \mathbf{s}^{(n-1)} = \mathbf{1}$  and  $\bar{\mathbf{s}}^{(n-1)T} \mathbf{s}^{(n-1)} \geq (1 - E_R/2)L$ . Let  $x_l^{(n-1)} = \rho_l e^{j\psi_l}$ , then  $(\mathbf{B}^{(n-1)} \mathbf{s}^{(n-1)})_l$ , the  $l$ -th element of  $\mathbf{B}^{(n-1)} \mathbf{s}^{(n-1)}$ , should be equal to 1. That is,

$$(\mathbf{B}^{(n-1)} \mathbf{s}^{(n-1)})_l = \text{Re}\{x_l^{(n-1)}\} \cos(\gamma_l^{(n-1)}) + \text{Im}\{x_l^{(n-1)}\} \sin(\gamma_l^{(n-1)}) \quad (4.32)$$

$$= \rho_l \cos(\psi_l) \cos(\gamma_l^{(n-1)}) + \rho_l \sin(\psi_l) \sin(\gamma_l^{(n-1)}) \quad (4.33)$$

$$= 1 \quad (4.34)$$

where  $\gamma_l^{(n)} = 2 \arg(x_l^{(n-1)}) - \delta x_l^{(n-1)}$ . This implies

$$\rho_l = \frac{1}{\cos(\psi_l) \cos(\gamma_l^{(n-1)}) + \sin(\psi_l) \sin(\gamma_l^{(n-1)})} \quad (4.35)$$

Note that  $\mathbf{s}^{(n-1)}$  belongs to the feasible set of  $CP^{(n)}$  if and only if  $\mathbf{B}^{(n)} \mathbf{s}^{(n-1)} = \mathbf{1}$  and  $\bar{\mathbf{s}}^{(n)T} \mathbf{s}^{(n-1)} \geq (1 - E_R/2)L$ . We have

$$(\mathbf{B}^{(n)} \mathbf{s}^{(n-1)})_l = \rho_l \cos(\psi_l) \cos(\gamma_l^{(n)}) + \rho_l \sin(\psi_l) \sin(\gamma_l^{(n)}) \quad (4.36)$$

$$= \rho_l \cos(\psi_l - \gamma_l^{(n)}) \quad (4.37)$$

$$= \rho_l \cos(\psi_l - 2\psi_l + \gamma_l^{(n-1)}) \quad (4.38)$$

$$= \rho_l \cos(\psi_l - \gamma_l^{(n-1)}) \quad (4.39)$$

$$= \rho_l \cos(\psi_l) \cos(\gamma_l^{(n-1)}) + \rho_l \sin(\psi_l) \sin(\gamma_l^{(n-1)}) \quad (4.40)$$

$$= 1 \quad (4.41)$$

<sup>1</sup>For a formal proof of this, see [97]

To show  $\bar{\mathbf{s}}^{(n)T} \mathbf{s}^{(n-1)} \geq (1 - E_R/2)L$ , let  $\bar{\mathbf{x}}$  denote the complex version of  $\bar{\mathbf{s}}$ , that is,  $\bar{\mathbf{s}} = [\text{Re}\{\bar{\mathbf{x}}\}^T \text{Im}\{\bar{\mathbf{x}}\}^T]^T$ . Then we have

$$(1 - E_R/2)L \leq \bar{\mathbf{s}}^{(n-1)T} \mathbf{s}^{(n-1)} \quad (4.42)$$

$$= \text{Re}\{\bar{\mathbf{x}}^{(n-1)H} \mathbf{x}^{(n-1)}\} \quad (4.43)$$

$$= \text{Re}\left\{\sum_l^L \bar{x}_l^{*(n-1)} \rho_l e^{j\psi_l}\right\} \quad (4.44)$$

$$\leq \left|\sum_l^L \bar{x}_l^{*(n-1)} \rho_l e^{j\psi_l}\right| \quad (4.45)$$

$$\leq \sum_l^L \left|\bar{x}_l^{*(n-1)} \rho_l e^{j\psi_l}\right| \quad (4.46)$$

$$\leq \sum_l^L \left|\bar{x}_l^{*(n-1)}\right| \rho_l \quad (4.47)$$

$$= \sum_l^L |\bar{x}_l^{*(n-1)}| e^{-j\psi_l} \rho_l e^{j\psi_l} \quad (4.48)$$

$$= \sum_l^L \bar{x}_l^{*(n)} \rho_l e^{j\psi_l} \quad (4.49)$$

$$= \text{Re}\{\bar{\mathbf{x}}^{(n)H} \mathbf{x}^{(n-1)}\} \quad (4.50)$$

$$= \bar{\mathbf{s}}^{(n)T} \mathbf{s}^{(n-1)} \quad (4.51)$$

Note that the equality between (4.48) and (4.49) holds because we define  $\bar{\mathbf{s}}^{(n)}$  such that  $\arg(\bar{\mathbf{F}}^H \bar{\mathbf{y}}) = \arg(\mathbf{x}^{(n-1)})$ . Eqs. (4.41) and (4.51) confirm  $\mathbf{B}^{(n)} \mathbf{s}^{(n-1)} = \mathbf{1}$  and  $\bar{\mathbf{s}}^{(n)T} \mathbf{s}^{(n-1)} \geq (1 - E_R/2)L$ .  $\square$

Lemma 4.4.1 proves that the feasible set of each iteration is updated such that it contains the optimal solution of the optimization problem at the previous iteration step. If  $|\mathbf{x}^{(n)}| = \mathbf{1}$ , then the constraints of the next problem  $CP^{(n+1)}$  are the same as problem  $CP^{(n)}$ , which means  $\mathbf{x}^{(n+1)} = \mathbf{x}^{(n)}$  and, hence, the algorithm converges. Lemma 4.4.3 further establishes that the cost function sequence is in fact non-increasing and converges. This procedure is visually illustrated in Fig. 4.2.

Now we focus on how to solve the optimization problem (4.29) at each iteration step. Note that the problem (4.29) is a convex quadratic minimization with linear equality constraints. Using the optimality conditions for problem (4.29), the sufficient and necessary Karush-Kuhn-Tucker (KKT) conditions [98] of (4.29) give the following.

$$2(\mathbf{R} + \lambda \mathbf{I}) \mathbf{s}^{(n)} + \mathbf{B}^{(n)T} \mathbf{v}^{(n)} - \mu^{(n)} \bar{\mathbf{s}} = \mathbf{0} \quad (4.52)$$

$$\mathbf{B}^{(n)} \mathbf{s}^{(n)} = \mathbf{1} \quad (4.53)$$

$$\mu^{(n)} (\bar{\mathbf{s}}^{(n)T} \mathbf{s}^{(n)} - (1 - E_R/2)L) = 0 \quad (4.54)$$

$$\bar{\mathbf{s}}^{(n)T} \mathbf{s}^{(n)} - (1 - E_R/2)L \geq 0 \quad (4.55)$$

$$\mu^{(n)} \geq 0 \quad (4.56)$$

We can directly solve these equations to find  $\mathbf{s}^{(n)}$ ,  $\mathbf{v}^{(n)}$  and  $\mu^{(n)}$ . The complementary slackness condition (4.54) implies that either  $\mu^{(n)} = 0$  or  $\bar{\mathbf{s}}^{(n)T} \mathbf{s}^{(n)} - (1 - E_R/2)L = 0$  must be satisfied. In the case of  $\mu^{(n)} = 0$ , from Eqs. (4.52) and (4.53), we have

$$\begin{bmatrix} \bar{\mathbf{R}} & \mathbf{B}^{(n)T} \\ \mathbf{B}^{(n)} & \mathbf{0} \end{bmatrix} \begin{bmatrix} \mathbf{s}^{(n)} \\ \mathbf{v}^{(n)} \end{bmatrix} = \begin{bmatrix} \mathbf{0} \\ \mathbf{1} \end{bmatrix} \quad (4.57)$$

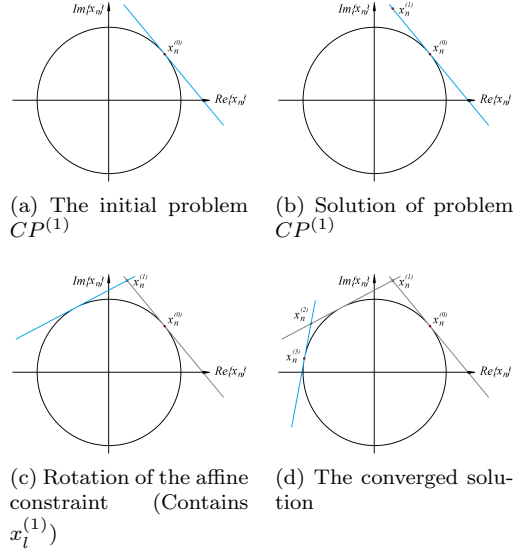


Figure 4.2: Illustration of the successive solutions of Eq. (4.29).

where  $\bar{\mathbf{R}} = 2(\mathbf{R} + \lambda \mathbf{I})$  and  $\mathbf{v}^{(n)} \in \mathbb{R}^{(L+1) \times 1}$  is the Lagrange multiplier associated with the equality constraints. Solving (4.57) by block elimination gives

$$\hat{\mathbf{s}}^{(n)} = \bar{\mathbf{R}}^{-1} \mathbf{B}^{(n)T} (\mathbf{B}^{(n)} \bar{\mathbf{R}}^{-1} \mathbf{B}^{(n)T})^{-1} \mathbf{1} \quad (4.58)$$

If  $\hat{\mathbf{s}}^{(n)}$  satisfies  $\bar{\mathbf{s}}^{(n)T} \hat{\mathbf{s}}^{(n)} - (1 - E_R/2)L \geq 0$ , then  $\mathbf{s}^{(n)} = \hat{\mathbf{s}}^{(n)}$  is the optimal solution of problem  $(CP^{(n)})$ . However, if  $\bar{\mathbf{s}}^{(n)T} \hat{\mathbf{s}}^{(n)} - (1 - E_R/2)L < 0$ , then  $\hat{\mathbf{s}}^{(n)}$  is not the solution since it violates (4.55). Thus,  $\mu^{(n)} = 0$  can not be valid and, therefore, it is the case that  $\bar{\mathbf{s}}^{(n)T} \mathbf{s}^{(n)} - (1 - E_R/2)L = 0$  must hold. In this case, the KKT conditions (4.52) through (4.54) are given in the matrix form by

$$\begin{bmatrix} \bar{\mathbf{R}} & \mathbf{B}^{(n)T} & -\bar{\mathbf{s}}^{(n)} \\ \mathbf{B}^{(n)} & \mathbf{0} & \mathbf{0} \\ -\bar{\mathbf{s}}^{(n)T} & \mathbf{0} & \mathbf{0} \end{bmatrix} \begin{bmatrix} \mathbf{s}^{(n)} \\ \mathbf{v}^{(n)} \\ \mu^{(n)} \end{bmatrix} = \begin{bmatrix} \mathbf{0} \\ \mathbf{1} \\ -(1 - E_R/2)L \end{bmatrix} \quad (4.59)$$

Using block elimination to solve (4.59) gives

$$\mathbf{s}^{(n)} = \mu^{(n)} \bar{\mathbf{R}}^{-1} (\mathbf{I} - \mathbf{B}^{(n)T} \hat{\mathbf{R}} \mathbf{B}^{(n)} \bar{\mathbf{R}}^{-1}) \bar{\mathbf{s}}^{(n)} + \hat{\mathbf{s}}^{(n)} \quad (4.60)$$

where

$$\hat{\mathbf{R}} = (\mathbf{B}^{(n)} \bar{\mathbf{R}}^{-1} \mathbf{B}^{(n)T})^{-1} \quad (4.61)$$

$$\mu^{(n)} = \frac{1}{\alpha^{(n)}} (\bar{\mathbf{s}}^{(n)T} \hat{\mathbf{s}}^{(n)} - (1 - E_R/2)L) \quad (4.62)$$

$$\alpha^{(n)} = - \begin{bmatrix} \bar{\mathbf{s}}^{(n)} \\ \mathbf{0} \end{bmatrix}^T \begin{bmatrix} \bar{\mathbf{R}} & \mathbf{B}^{(n)T} \\ \mathbf{B}^{(n)} & \mathbf{0} \end{bmatrix}^{-1} \begin{bmatrix} \bar{\mathbf{s}}^{(n)} \\ \mathbf{0} \end{bmatrix} \quad (4.63)$$

Note that (4.55) always holds since  $\bar{\mathbf{s}}^T \mathbf{s}^{(n)} - (1 - E_R/2)L = 0$  in this case. To confirm all KKT conditions are satisfied, we have to show the dual feasibility condition (4.56) holds. The following lemma proves this.

**Lemma 4.4.2.** *If  $\bar{\mathbf{s}}^T \hat{\mathbf{s}}^{(n)} - (1 - E_R/2)L < 0$  then  $\mu^{(n)} > 0$ .*

*Proof.* First, let

$$\mathbf{K} = \begin{bmatrix} \bar{\mathbf{R}} & \mathbf{B}^{(n)T} & -\bar{\mathbf{s}}^{(n)} \\ \mathbf{B}^{(n)} & \mathbf{0} & \mathbf{0} \\ -\bar{\mathbf{s}}^{(n)T} & \mathbf{0} & \mathbf{0} \end{bmatrix} \quad (4.64)$$

$$\mathbf{K}_{11} = \begin{bmatrix} \bar{\mathbf{R}} & \mathbf{B}^{(n)T} \\ \mathbf{B}^{(n)} & \mathbf{0} \end{bmatrix} \quad (4.65)$$

If  $\bar{\mathbf{s}}^{(n)}$  is linearly dependent on  $\mathbf{b}_1^{(n)}, \mathbf{b}_2^{(n)}, \dots, \mathbf{b}_{L+1}^{(n)}$  and  $\bar{\mathbf{s}}^T \hat{\mathbf{s}}^{(n)} - (1 - E_R/2)L < 0$ , then there will be no solution to  $CP^{(n)}$  which contradicts Lemma 4.4.1. Therefore,  $\mathbf{b}_1^{(n)}, \mathbf{b}_2^{(n)}, \dots, \mathbf{b}_{L+1}^{(n)}$ , and  $\bar{\mathbf{s}}$  must be linearly independent. Moreover, since  $\bar{\mathbf{R}}$  is positive definite, all the eigenvalues of  $\mathbf{K}$  are nonzero according to Theorem 2.1 in [99], which means  $\mathbf{K}$  is nonsingular. Since  $\mathbf{K}$  is nonsingular, the Schur complement of the block  $\mathbf{K}_{11}$  in  $\mathbf{K}$  is also non-singular (nonzero in our case) according to Section C.4 in [98] and equals to  $\alpha^{(n)}$ . This implies

$$\alpha^{(n)} \neq 0 \quad (4.66)$$

Using the block inverse to the matrix  $\mathbf{K}_{11}$ , Eq. (4.63) can be rewritten as

$$\alpha^{(n)} = -\bar{\mathbf{s}}^{(n)T} (\bar{\mathbf{R}}^{-1} - \bar{\mathbf{R}}^{-1} \mathbf{B}^{(n)T} \hat{\mathbf{R}} \mathbf{B}^{(n)} \bar{\mathbf{R}}^{-1}) \bar{\mathbf{s}}^{(n)} \quad (4.67)$$

$$= -\bar{\mathbf{s}}^{(n)T} \bar{\mathbf{R}}^{-\frac{1}{2}} (\mathbf{I} - \bar{\mathbf{R}}^{-\frac{1}{2}} \mathbf{B}^{(n)T} \hat{\mathbf{R}} \mathbf{B}^{(n)} \bar{\mathbf{R}}^{-\frac{1}{2}}) \bar{\mathbf{R}}^{-\frac{1}{2}} \bar{\mathbf{s}}^{(n)} \quad (4.68)$$

$$= -\mathbf{y}^T (\mathbf{I} - \bar{\mathbf{R}}^{-\frac{1}{2}} \mathbf{B}^{(n)T} (\mathbf{B}^{(n)} \bar{\mathbf{R}}^{-1} \mathbf{B}^{(n)T})^{-1} \mathbf{B}^{(n)} \bar{\mathbf{R}}^{-\frac{1}{2}}) \mathbf{y} \quad (4.69)$$

$$= -\mathbf{y}^T (\mathbf{I} - \mathbf{C}(\mathbf{C}^T \mathbf{C})^{-1} \mathbf{C}^T) \mathbf{y} \quad (4.70)$$

where  $\mathbf{y} = \bar{\mathbf{R}}^{-\frac{1}{2}} \bar{\mathbf{s}}^{(n)}$  and  $\mathbf{C} = \bar{\mathbf{R}}^{-\frac{1}{2}} \mathbf{B}^{(n)T}$ . Note that  $\mathbf{C}_p = \mathbf{C}(\mathbf{C}^T \mathbf{C})^{-1} \mathbf{C}^T$  is an idempotent matrix with eigenvalues of either 0 or 1 [100]. This implies that  $(\mathbf{I} - \mathbf{C}_p)$  is positive semidefinite. Therefore,

$$\alpha^{(n)} \leq 0 \quad (4.71)$$

Combining (4.66) and (4.71) implies that  $\alpha^{(n)} < 0$  and, hence,  $\mu^{(n)} > 0$ .  $\square$

**Computational Complexity:** Based on the computational cost of solving (4.59) in each iteration, the overall computational complexity of BIC is  $\mathcal{O}(FL^{2.373}) - \mathcal{O}(FL^3)$  [101] where  $F$  is the total number of iterations.

**Convergence Analysis:** The value of the objective function of the problem (4.16) as a function of the  $\mathbf{x}^{(n)}$ , i.e. the optimal solution of the QP at iteration  $n$ , is non-increasing in  $n$ . This is proven next.

**Lemma 4.4.3.** *Define  $g(\mathbf{s}) = \mathbf{s}^T (\mathbf{R} + \lambda \mathbf{I}) \mathbf{s}$ . Then*

$$g(\mathbf{s}^{(n-1)}) \geq g(\mathbf{s}^{(n)}) \quad (4.72)$$

*In other words, the sequence  $\{g(\mathbf{s}^{(n)})\}_{n=0}^{\infty}$  is non-increasing. Moreover, the sequence  $\{g(\mathbf{s}^{(n)})\}_{n=0}^{\infty}$  converges to a finite value  $g^*$ .*

*Proof.* Denote the feasible sets of  $CP^{(n-1)}$  and  $CP^{(n)}$  by  $\mathcal{F}_{n-1}$  and  $\mathcal{F}_n$ , respectively. From Lemma 4.4.1,  $\mathbf{s}^{(n-1)} \in \mathcal{F}_n$ . Since  $CP^{(n)}$  is a convex problem and  $\mathbf{s}^{(n)}$  is the optimal solution of  $CP^{(n)}$ ,

$$\mathbf{s}^{(n-1)T} (\mathbf{R} + \lambda \mathbf{I}) \mathbf{s}^{(n-1)} \geq \mathbf{s}^{(n)T} (\mathbf{R} + \lambda \mathbf{I}) \mathbf{s}^{(n)} \quad (4.73)$$

Therefore, the sequence  $\{g(\mathbf{s}^{(n)})\}_{n=0}^{\infty}$  is non-increasing. Since  $g(\mathbf{s}) \geq 0$  for all values of  $\mathbf{s}$ , it is bounded below. Hence, it converges to a finite value  $g^*$  according to the monotone convergence theorem [102].  $\square$

Fig. 4.3 verifies the cost function is non-increasing and converges. We plot the cost function in dB (blue line) and actual values (red line). The blue and red lines clearly show the non-increasing property and convergence of the proposed algorithm, respectively.

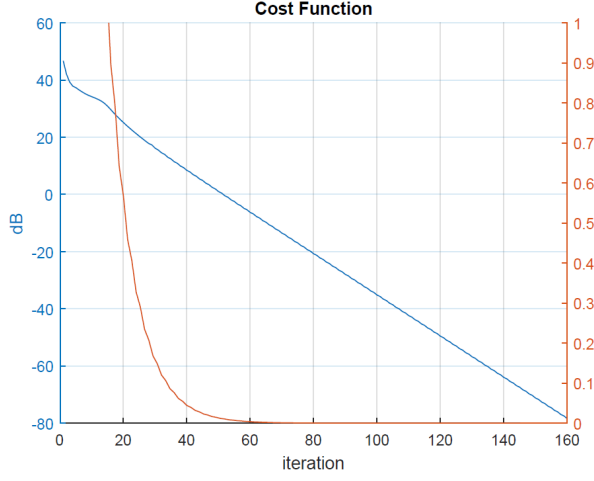


Figure 4.3: Value of cost function vs. iteration (red curve for the linear scale and blue curve for the log scale).

#### 4.4.3 Special Case: Nullforming Beampattern Design

Null forming beampattern design can be seen as a special case of our full beampattern design. However, unlike the problem formulation in (4.10), the goal of null forming beampattern design is to form a beampattern with nulls in desired directions denoted by  $\{\theta_k\}_{k=1}^K$ . Here, the objective function can be defined by

$$f(\mathbf{x}) = \sum_{p=-\frac{N}{2}}^{\frac{N}{2}-1} \|\mathbf{A}_p \mathbf{W}_p \mathbf{x}\|_2^2 \quad (4.74)$$

$$= \mathbf{x}^H \mathbf{V} \mathbf{x} \quad (4.75)$$

where  $\mathbf{V}$  is expressed as

$$\mathbf{V} = \sum_{p=-\frac{N}{2}}^{\frac{N}{2}-1} \mathbf{W}_p^H \mathbf{A}_p^H \mathbf{A}_p \mathbf{W}_p \quad (4.76)$$

Therefore, the minimization problem can be formulated as

$$\begin{cases} \min_{\mathbf{x}} & \mathbf{x}^H \mathbf{V} \mathbf{x} \\ \text{s.t.} & |\mathbf{x}| = \mathbf{1} \\ & \|\bar{\mathbf{F}}^H \bar{\mathbf{y}} - \mathbf{x}\|_2^2 \leq E_R \end{cases} \quad (4.77)$$

In this case, the optimization problem reduces to problem  $CP^{(n)}$  in (4.29) with  $\mathbf{R}$  and  $\mathbf{s}$  redefined as:

$$\mathbf{R} = \begin{bmatrix} \text{Re}\{\mathbf{V}\} & -\text{Im}\{\mathbf{V}\} \\ \text{Im}\{\mathbf{V}\} & \text{Re}\{\mathbf{V}\} \end{bmatrix} \quad (4.78)$$

$$\mathbf{s} = \begin{bmatrix} \text{Re}\{\mathbf{x}\} \\ \text{Im}\{\mathbf{x}\} \end{bmatrix} \quad (4.79)$$

Since  $\mathbf{V}$  is positive semi-definite and there are no linear terms in the objective function (i.e.  $\mathbf{q} = \mathbf{0}$  and  $r = 0$ ), then all the lemmas in Section 4.4.2 hold.

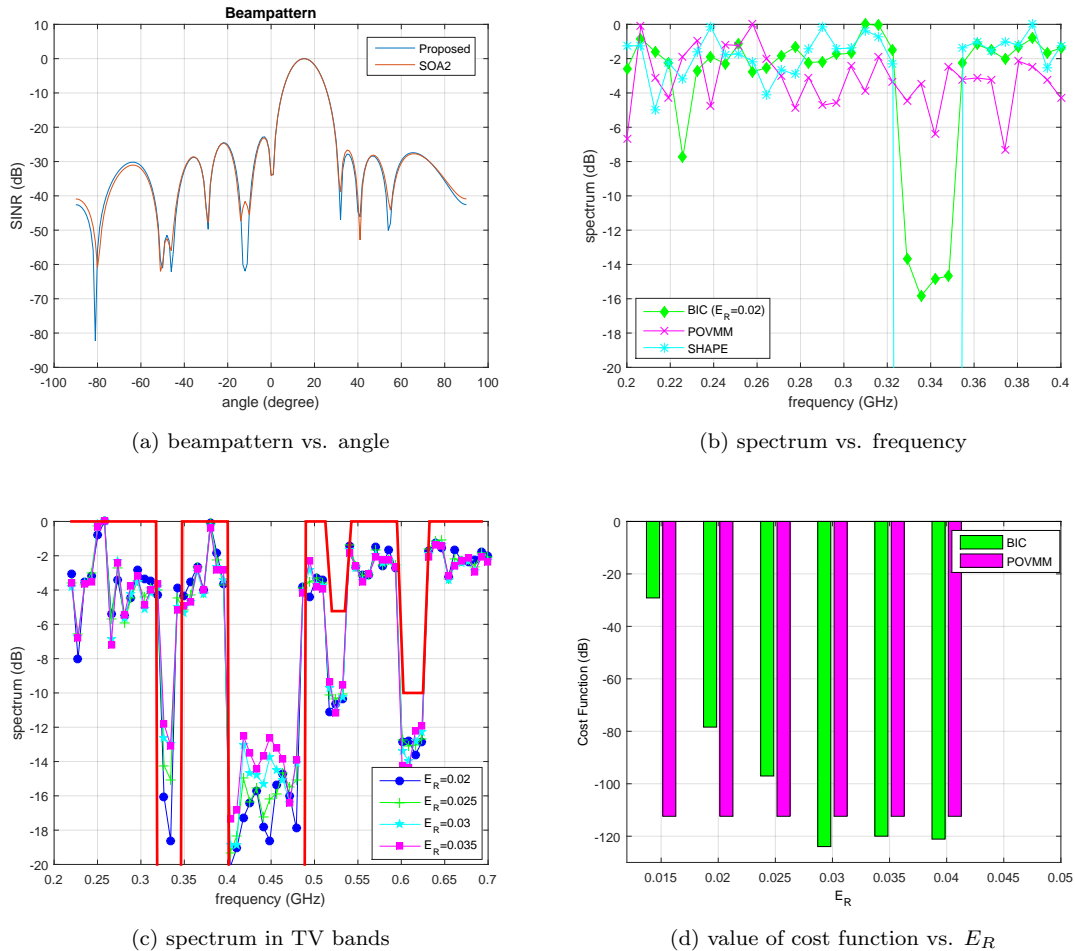


Figure 4.4: Nullforming beampattern design

## 4.5 Results and Discussions

We examine the performance of the proposed BIC by comparing it against the following well-known methods:

- **Phase-only variable metric method (POVMM) [72]:** POVMM performs null forming beampattern design by optimizing phases of the waveform under the constant modulus constraint but no spectral constraint is involved.
- **SHAPE [87]:** The SHAPE algorithm is a computationally efficient method of designing sequences with desired spectrum shapes. In particular, the spectral shape is optimized as a cost function subject to the constant modulus constraint but the resulting beampattern is an outcome (not explicitly controlled).
- **Wideband beampattern formation via iterative techniques (WBFIT) [83]:** The WBFIT synthesizes wideband MIMO beampattern under the constant modulus or low PAR. They first find the Fourier transformed waveform in the frequency domain and then fit the DFT of the waveform to the result of the first step subject to the enforced PAR constraint.

### 4.5.1 Nullforming Beampattern Design

We compare the proposed BIC to the state-of-the-art phase-only variable metric method (POVMM) method [72] and the SHAPE algorithm [87]. The experimental set up is as follows: We simulate a linear MIMO radar antenna array of  $M = 16$  elements with half-wavelength spacing and number of time samples  $N = 32$ . We consider  $K = 3$ ,  $\theta = [10^\circ, 40^\circ, 120^\circ]$ . We assume a carrier frequency of  $f_c = 300$  MHz and we have access to the 225-328.6 MHz and 335-400.15 MHz bands allocated for the U.S. Federal Government. We then place a notch in the band 328.6-335 MHz.

Fig. 4.4 shows the results for nullforming beampattern of BIC versus POVMM and SHAPE. Fig. 4.4a, we plot the resulting beampattern versus the angle. Note that the BIC and POVMM have nulls in the desired angles while the SHAPE captures the spectral constraint without beampattern control. On the other hand, Fig. 4.4b plots the spectrum versus the frequency. Here, BIC and SHAPE effectively suppress the energy in the frequency bands where the transmission should be mitigated. Unsurprisingly, POVMM does not provide the desired suppression in the frequency bands of interest because it is not designed for the same. In summary, only the proposed BIC enables the desired spatio-spectral control.

In Fig. 4.4c, we investigate a more practical scenario. We assume we have access to licensed television broadcasts (UHF) that occur from 470 to 698 MHz as well as the 225-328.6 MHz and 335-400.15 MHz bands as in Fig. 4.4a. Each television station is allocated 6 MHz of bandwidth and we assume there are 7 stations are licensed for operation (Ch. 21-23, 512-536 MHz and Ch. 36-39, 602-626 MHz). We plot the spectrum as achieved by different methods with different threshold ( $E_R$ ) values in Fig. 4.4c and as expected a smaller threshold ( $E_R$  value) leads to a tighter spectral constraint.

It is also shown in Fig. 4.4c that the spectral constraint can be set to incorporate the information of the distance of a TV station/wireless interferer to the radar. In particular the results in Fig. 4.4c assume that the stations of Ch. 36-39 are closer to the radar than Ch. 21-23.  $\bar{y}$  in (4.77) is appropriately set (see red curve in Fig. 4.4c) to control the relative importance of frequency bands.

In Fig. 4.4d, we show the cost function value corresponding to POVMM and the proposed BIC (recall, they optimize the same cost function in the nullforming case). The BIC method achieves similar cost function values or lower when  $E_R \geq 0.03$ . This is particularly remarkable because BIC additionally enforces the spectral constraint.

### 4.5.2 Full Beampattern Design

For wideband beampattern design, we compare BIC to the state-of-the-art WBFIT method [83]. The experimental set-up used in Fig. 4.5 and Fig. 4.6 is following. The number of transmit antennas  $M = 10$ , the number of time samples  $N = 32$ , the carrier frequency of the transmit signal  $f_c = 1$  GHz and the bandwidth  $B = 200$  MHz and the spatial angle is divided into  $K = 180$  grid points.

In Fig. 4.5, we place a notch in the band 910-932 MHz and consider the following desired transmit beampattern

$$d(\theta, f) = \begin{cases} 1 & \theta = [95^\circ, 120^\circ] \\ 0 & \text{Otherwise.} \end{cases} \quad (4.80)$$

Fig. 4.5 shows the angle-frequency plot of the beampattern for WBFIT method (no spectral constraint) and BIC with the spectral constraint ( $E_R = 0.01$ ). The BIC method is able to keep the energy of the waveform in particular frequency band low enough as well as achieve higher suppression at the undesired angles compared to WBFIT.

In Fig. 4.6, we simulate a more challenging practical scenario. We assume that the beampattern should be suppressed at the angles of  $40^\circ$  through  $80^\circ$  in the frequency band [943.75 MHz, 981.25 MHz] and at  $120^\circ$  through  $160^\circ$  in [962.5 MHz, 1,000 MHz], that is,

$$d(\theta, f) = \begin{cases} 0 & \theta = [40^\circ, 80^\circ] \text{ and } f = [943.75, 981.25] \\ 0 & \theta = [120^\circ, 160^\circ] \text{ and } f = [962.5, 1000] \\ 1 & \text{Otherwise.} \end{cases} \quad (4.81)$$

This ideally appears as black boxes in the angle-frequency beampattern plots. We also assume that transmission should be restricted at all directions in the frequency band [1.025 GHz, 1.0625 GHz]. This restriction can be performed by the spectral constraint. First, as shown in Fig. 4.6b, since WBFIT does not have the spectral constraint, the notch of frequency band [1.025 GHz, 1.0625 GHz] does not appear. Second, the black boxes are not seen so clearly in Fig. 4.6b. Lastly, WBFIT suppresses the energy of the waveform unnecessarily in the frequency band where we do not have any restriction (e.g. [1.0625 GHz, 1.1 GHz]). On the other hand, the proposed BIC effectively suppresses and restricts the transmitted energy in the desired frequency bands and angles and generate enough power elsewhere.

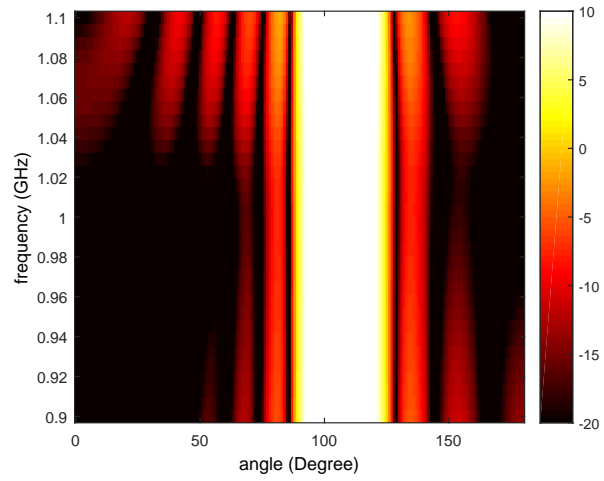
Table 4.1: Converged cost function values in dB

Method	cost function (dB)
Unconstrained	15.4681
WBFIT	34.7744
BIC ( $E_R = 0.01$ )	32.6461
BIC ( $E_R = 0.02$ )	31.3286
BIC ( $E_R = 0.03$ )	30.8468

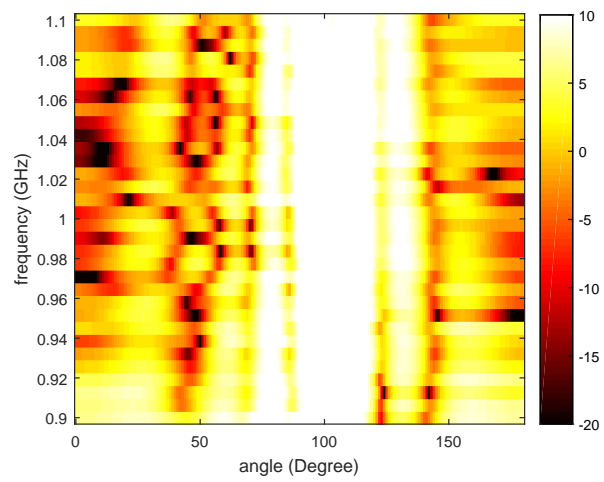
Finally, we compare values of the cost function of each algorithm for the same scenario in (4.81) and the results are reported in Table 4.1. In Table 4.1, unconstrained wideband beampattern design (not even a constant modulus constraint) plays the role of a lower bound. BIC outperforms WBFIT even as it incorporates an additional spectral constraint.

## 4.6 Conclusion

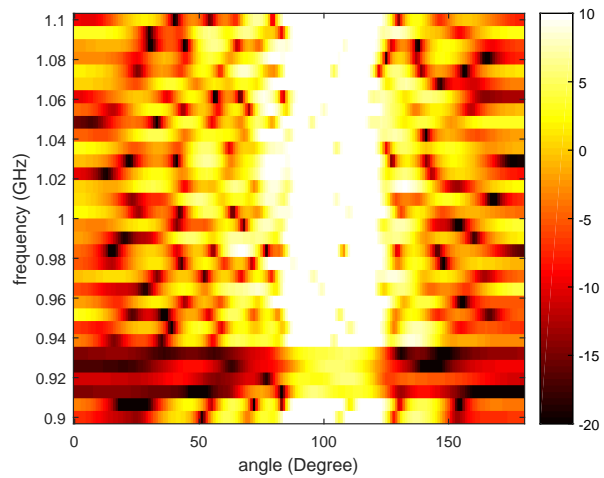
Our work achieves tractable spatio-spectral beampattern design by waveform optimization for MIMO radar in the presence of constant modulus and spectral constraints. The central idea of our analytical contribution is to successively achieve constant modulus (at convergence), while solving a quadratic program with linear equality and inequality constraints in each step of the sequence. Because each problem in the sequence has a closed form, this makes our method computationally attractive. We establish new analytical properties of the BIC algorithm such as non-increasing cost function in each iteration and guaranteed convergence. Further, we show experimentally that the proposed BIC can achieve superior beampattern accuracy compared to many state-of-the-art methods even as BIC solves a spectrally constrained problem. Future work could consider the incorporation of additional constraints such as waveform similarity [90, 103] and explore further optimality properties of the BIC solution.



(a)



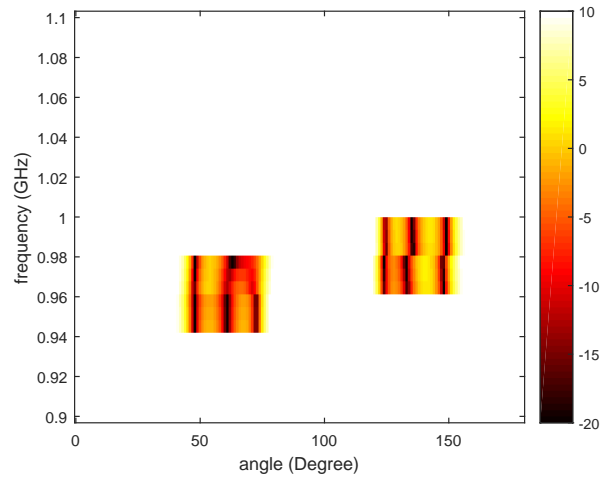
(b)



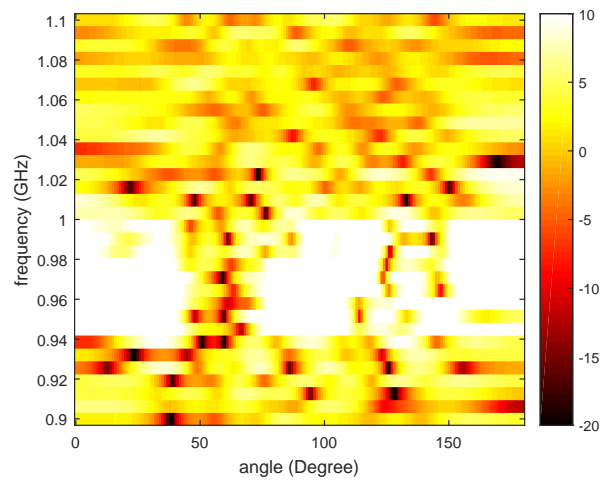
(c)

Figure 4.5: Plot of the beam pattern. (a) unconstrained (b) WBFIT method (c) BIC (Proposed method)

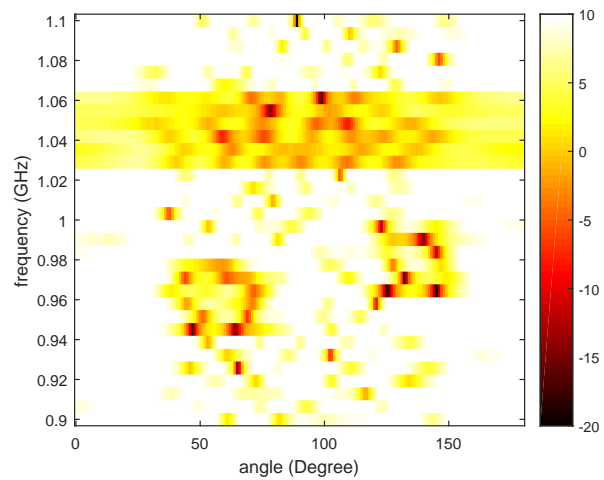
DISTRIBUTION A: Distribution approved for public release.



(a)



(b)



(c)

Figure 4.6: Plot of the beam pattern. (a) unconstrained (b) WBFIT method (c) BIC (Proposed method)

DISTRIBUTION A: Distribution approved for public release.

# Bibliography

- [1] L. K. Patton, S. W. Frost, and B. D. Rigling, "Efficient design of radar waveforms for optimised detection in coloured noise," *IET Radar, Sonar & Navigation*, vol. 6, no. 1, pp. 21–29, Jan. 2012.
- [2] M. R. Bell, "Information theory and radar waveform design," *Information Theory, IEEE Transactions on*, vol. 39, no. 5, pp. 1578–1597, Sept. 1993.
- [3] Y. Yang and R. S. Blum, "Waveform design for MIMO radar based on mutual information and minimum mean-square error estimation," in *Information Sciences and Systems, 2006 40th Annual Conference on*. 2006, pp. 111–116, IEEE.
- [4] G. Wang and Y. Lu, "Sparse frequency waveform design for MIMO radar," *Progress In Electromagnetics Research B*, vol. 20, pp. 19–32, 2010.
- [5] F. Gini, *Waveform design and diversity for advanced radar systems*, The Institution of Engineering and Technology, 2012.
- [6] J. D. Wolf, G. M. Lee, and C. E. Suvo, "Radar waveform synthesis by mean square optimization techniques," *Aerospace and Electronic Systems, IEEE Transactions on*, , no. 4, pp. 611–619, 1969.
- [7] A. Aubry, A. De Maio, B. Jiang, and S. Zhang, "Ambiguity function shaping for cognitive radar via complex quartic optimization," *Signal Processing, IEEE Transactions on*, vol. 61, no. 22, pp. 5603–5619, Nov. 2013.
- [8] A. Leshem, O. Naparstek, and A. Nehorai, "Information theoretic adaptive radar waveform design for multiple extended targets," *Selected Topics in Signal Processing, IEEE Journal of*, vol. 1, no. 1, pp. 42–55, 2007.
- [9] S. Sen and A. Nehorai, "OFDM MIMO radar with mutual-information waveform design for low-grazing angle tracking," *Signal Processing, IEEE Transactions on*, vol. 58, no. 6, pp. 3152–3162, 2010.
- [10] Y. Yang and R. S. Blum, "MIMO radar waveform design based on mutual information and minimum mean-square error estimation," *Aerospace and Electronic Systems, IEEE Transactions on*, vol. 43, no. 1, pp. 330–343, 2007.
- [11] Y. Wang, X. Wang, H. Liu, and Z. Luo, "On the design of constant modulus probing signals for MIMO radar," *Signal Processing, IEEE Transactions on*, vol. 60, no. 8, pp. 4432–4438, Aug. 2012.
- [12] H. Deng, L. Guo, B. Himed, Tan Ma, and Z. Geng, "Waveform optimization for transmit beamforming with MIMO radar antenna arrays," *Antennas and Propagation, IEEE Transactions on*, pp. 543–552, Dec. 2014.
- [13] H. Zang, H.i Liu, S. Zhou, and X. Wang, "MIMO radar waveform design involving receiving beamforming," in *Radar Conference (Radar), 2014 International*. IEEE, Oct. 2014, pp. 1–4.
- [14] L. K. Patton, *On the Satisfaction of Modulus and Ambiguity Function Constraints in Radar Waveform Optimization for Detection*, Ph.D. thesis, Wright State University, June 2009.
- [15] G. Cui, H. Li, and M. Rangaswamy, "MIMO Radar Waveform Design With Constant Modulus and Similarity Constraints," *IEEE Transactions on Signal Processing*, vol. 62, no. 2, pp. 343–353, January 2014.
- [16] B. Friedlander, "Waveform design for MIMO radars," *Aerospace and Electronic Systems, IEEE Transactions on*, vol. 43, no. 3, pp. 1227–1238, July 2007.
- [17] Z. Luo, W. Ma, A. So, Y. Ye, and S. Zhang, "Semidefinite relaxation of quadratic optimization problems," *Signal Processing Magazine, IEEE*, vol. 27, no. 3, pp. 20–34, 2010.
- [18] Z. Luo and T. Chang, "SDP relaxation of homogeneous quadratic optimization: approximation bounds and applications," *Convex Optimization in Signal Processing and Communications*, p. 117, 2010.
- [19] G. Cui, H. Li, and M. Rangaswamy, "Waveform design for MIMO radar with constant modulus and similarity constraints," in *Radar Conference, 2014 IEEE*. IEEE, Jan. 2014, pp. 0354–0359.
- [20] A. Aubry, A. De Maio, M. Piezzo, A. Farina, and M. Wicks, "Cognitive design of the receive filter and transmitted phase code in reverberating environment," *IET Radar, Sonar & Navigation*, vol. 6, no. 9, pp. 822–833, Dec. 2012.
- [21] O. Aldayel, V. Monga, and M. Rangaswamy, "SQR: Successive QCQP Refinement for MIMO Radar Waveform Design Under Practical Constraints," Tech. Rep., Pennsylvania State University, 2015, Available at: <http://www.personal.psu.edu/osa105/TechReport.pdf>.

- [22] A. Aubry, A. De Maio, M. Piezzo, and A. Farina, "Radar waveform design in a spectrally crowded environment via nonconvex quadratic optimization," *Aerospace and Electronic Systems, IEEE Transactions on*, vol. 50, no. 2, pp. 1138–1152, 2014.
- [23] A. Aubry, A. De Maio, M. Piezzo, M. M. Naghsh, M. Soltanalian, and P. Stoica, "Cognitive radar waveform design for spectral coexistence in signal-dependent interference," in *Radar Conference, 2014 IEEE*. IEEE, 2014, pp. 0474–0478.
- [24] S. Zhang and Y. Huang, "Complex quadratic optimization and semidefinite programming," *SIAM Journal on Optimization*, vol. 16, no. 3, pp. 871–890, 2006.
- [25] M. Sousa Lobo, L. Vandenberghe, S. Boyd, and H. Lebet, "Applications of second-order cone programming," *Linear algebra and its applications*, vol. 284, no. 1, pp. 193–228, 1998.
- [26] S. Boyd and L. Vandenberghe, *Convex Optimization*, Cambridge University Press, 2004.
- [27] S. Boyd and J. Mattingley, "Branch and bound methods," *Notes for EE364b, Stanford University*, pp. 2006–07, 2007.
- [28] W. Dinkelbach, "On Nonlinear Fractional Programming," *Management Science*, vol. 13, no. 7, pp. 492–498, March 1967.
- [29] A. Zhang and S. Hayashi, "Celis-Dennis-Tapia Based Approach to Quadratic Fractional Programming Problems with Two Quadratic Constraints," Tech. Rep., Kyoto University, 2010, [http://www.amp.i.kyoto-u.ac.jp/tecrep/ps\\_file/2010/2010-012.pdf](http://www.amp.i.kyoto-u.ac.jp/tecrep/ps_file/2010/2010-012.pdf).
- [30] M. Salahi and S. Fallahi, "On the Quadratic Fractional Optimization with a Strictly Convex Quadratic Constraint," *Kybernetika*, vol. 51, no. 2, pp. 293–308, 2015.
- [31] S. Schaible, "Fractional Programming II, On Dinkelbach's Algorithm," *Management Science*, vol. 22, no. 8, pp. 868–873, April 1976.
- [32] A. De Maio, S. De Nicola, Y. Huang, Z. Luo, and S. Zhang, "Design of phase codes for radar performance optimization with a similarity constraint," *Signal Processing, IEEE Transactions on*, vol. 57, no. 2, pp. 610–621, 2009.
- [33] T. C. Cheston and J. Frank, "Phased array radar antennas," *Radar Handbook*, pp. 7–1, 1990.
- [34] H. Lebet and S. Boyd, "Antenna array pattern synthesis via convex optimization," *Signal Processing, IEEE Transactions on*, vol. 45, no. 3, pp. 526–532, Mar. 1997.
- [35] D. R. Scholnik and J. O. Coleman, "Optimal design of wideband array patterns," in *Radar Conference, 2000. The Record of the IEEE 2000 International*. IEEE, 2000, pp. 172–177.
- [36] G. Cardone, G. Cincotti, and M. Pappalardo, "Design of wide-band arrays for low side-lobe level beam patterns by simulated annealing," *Ultrasonics, Ferroelectrics, and Frequency Control, IEEE Transactions on*, vol. 49, no. 8, pp. 1050–1059, Aug. 2002.
- [37] G. S. Antonio and D. R. Fuhrmann, "Beampattern synthesis for wideband MIMO radar systems," in *Computational Advances in Multi-Sensor Adaptive Processing, 2005 1st IEEE International Workshop on*. IEEE, Dec. 2005, pp. 105–108.
- [38] J. Li, Y. Xie, P. Stoica, X. Zheng, and J. Ward, "Beampattern synthesis via a matrix approach for signal power estimation," *Signal Processing, IEEE Transactions on*, vol. 55, no. 12, pp. 5643–5657, Dec. 2007.
- [39] L. Guo, H. Deng, B. Himed, T. Ma, and Z. Geng, "Waveform optimization for transmit beamforming with MIMO radar antenna arrays," *Antennas and Propagation, IEEE Transactions on*, vol. 63, no. 2, pp. 543–552, Feb. 2015.
- [40] S. Sen, "Constant-envelope waveform design for optimal target-detection and autocorrelation performances," in *Acoustics, Speech and Signal Processing (ICASSP), 2013 IEEE International Conference on*. IEEE, May 2013, pp. 3851–3855.
- [41] W. Rowe, P. Stoica, and J. Li, "Spectrally Constrained Waveform Design [sp Tips&Tricks]," *Signal Processing Magazine, IEEE*, vol. 31, no. 3, pp. 157–162, May 2014.
- [42] S. Ahmed and M. S. Alouini, "MIMO radar transmit beampattern design without synthesising the covariance matrix," *Signal Processing, IEEE Transactions on*, vol. 62, no. 9, pp. 2278–2289, May 2014.
- [43] X. Zhang, Z. He, L. Rayman-Bacchus, and J. Yan, "MIMO radar transmit beampattern matching design," *Signal Processing, IEEE Transactions on*, vol. 63, no. 8, pp. 2049–2056, Apr. 2015.
- [44] C. Pan, J. Benesty, and J. Chen, "Design of directivity patterns with a unique null of maximum multiplicity," *IEEE/ACM Transactions on Audio, Speech, and Language Processing*, vol. 24, no. 2, pp. 226–235, Feb. 2016.
- [45] Z. Chen, H. Li, G. Cui, and M. Rangaswamy, "Adaptive transmit and receive beamforming for interference mitigation," *Signal Processing Letters, IEEE*, vol. 21, no. 2, pp. 235–239, Feb. 2014.
- [46] W. Roberts, J. Li, P. Stoica, and Xumin XZhu, "MIMO radar receiver design," in *Radar Conference, 2008. RADAR'08. IEEE*. IEEE, May 2008, pp. 1–6.
- [47] P. Stoica, J. Li, and X. Zhu, "Waveform synthesis for diversity-based transmit beampattern design," *Signal Processing, IEEE Transactions on*, vol. 56, no. 6, pp. 2593–2598, June 2008.
- [48] G. Hua and S. S. Abeysekera, "MIMO radar transmit beampattern design with ripple and transition band control," *Signal Processing, IEEE Transactions on*, vol. 61, no. 11, pp. 2963–2974, June 2013.

- [49] J. Lipor, S. Ahmed, and M. S. Alouini, "Fourier-based transmit beampattern design using MIMO radar," *Signal Processing, IEEE Transactions on*, vol. 62, no. 9, pp. 2226–2235, May 2014.
- [50] H. Xu, R. S. Blum, J. Wang, and J. Yuan, "Colocated MIMO radar waveform design for transmit beampattern formation," *Aerospace and Electronic Systems, IEEE Transactions on*, vol. 51, no. 2, pp. 1558–1568, Apr. 2015.
- [51] Hao He, Petre Stoica, and Jian Li, "Wideband MIMO systems: signal design for transmit beampattern synthesis," *Signal Processing, IEEE Transactions on*, vol. 59, no. 2, pp. 618–628, Feb. 2011.
- [52] L. K. Patton and B. D. Rigling, "Modulus constraints in adaptive radar waveform design," in *Radar Conference, 2008. RADAR'08. IEEE*. IEEE, May 2008, pp. 1–6.
- [53] T. Guo and R. Qiu, "OFDM waveform design compromising spectral nulling, side-lobe suppression and range resolution," in *Radar Conference, 2014 IEEE*. IEEE, May 2014, pp. 1424–1429.
- [54] Steven M Sussman, "Least-square synthesis of radar ambiguity functions," *Information Theory, IRE Transactions on*, vol. 8, no. 3, pp. 246–254, Apr. 1962.
- [55] R. W. Gerchber and W. O. Saxton, "Phase determination from image and diffraction plane pictures in electron-microscope," *Optik*, vol. 34, no. 3, pp. 275, Jan. 1971.
- [56] J. Dattorro, *Convex optimization & Euclidean distance geometry*, Lulu. com, 2010.
- [57] N. J. Higham and S. H. Cheng, "Modifying the inertia of matrices arising in optimization," *Linear Algebra and its Applications*, vol. 275, pp. 261–279, May 1998.
- [58] O. Aldayel, V. Monga, and M. Rangaswamy, "Successive qcqp refinement for mimo radar waveform design under practical constraints," *Signal Processing, IEEE Transactions on*, vol. 64, no. 14, pp. 3760–3773, July 2016.
- [59] J. Liang, H. C. So, J. Li, and A. Farina, "Unimodular sequence design based on alternating direction method of multipliers," *IEEE Transactions on Signal Processing*, vol. 64, no. 20, pp. 5367–5381, 2016.
- [60] C. Chen and P. P. Vaidyanathan, "MIMO radar waveform optimization with prior information of the extended target and clutter," *Signal Processing, IEEE Transactions on*, vol. 57, no. 9, pp. 3533–3544, Sept. 2009.
- [61] A. Aubry, A. De Maio, and A. Farina, "Radar Waveform Design in a Spectrally Crowded Environment Via Nonconvex Quadratic Optimization," *IEEE Trans. Aerosp. Electron. Syst.*, vol. 50, no. 2, pp. 1138–1152, April 2014.
- [62] A. Aubry, A. De Maio, M. Piezzo, M. M. Naghsh, M. Soltanalian, and P. Stoica, "Cognitive Radar Waveform Design for Spectral Coexistence in Signal-Dependent Interference," in *IEEE Radar Conference*, May 2014, pp. 474–478.
- [63] K. D. Shepherd and R. A. Romero, "Radar Waveform Design in Active Communications Channel," in *Conference Record of The Forty-Seventh Asilomar Conference on Signals, Systems and Computers*, November 2013, vol. 1, pp. 1515–1519.
- [64] T. Guo and R. Qiu, "OFDM Waveform Design Compromising Spectral Nulling, Side-lobe Suppression and Range Resolution," in *IEEE Radar Conference*, May 2014, pp. 1424–1429.
- [65] F. Xin, J. Wang, B. Wang, and X. Song, "Waveform Design for Cognitive Radar Based on Information Theory," in *Multisensor Fusion and Information Integration for Intelligent Systems (MFI), 2014 International Conference on*, September 2014, pp. 1–8.
- [66] W. Huleihel, J. Tabrikian, and R. Shavit, "Optimal Adaptive Waveform Design for Cognitive MIMO Radar," *IEEE Trans. Signal Processing*, vol. 61, no. 20, pp. 5075–5089, October 2013.
- [67] B. Tang, J. Tang, and Y. Peng, "MIMO Radar Waveform Design in Colored Noise Based on Information Theory," *IEEE Trans. Signal Processing*, vol. 58, no. 9, pp. 4684–4697, September 2010.
- [68] S. Amuru, R. M. Buehrer, R. Tandon, and S. Sodagari, "MIMO radar waveform design to support spectrum sharing," in *2013 IEEE Military Communications Conference*, 2013.
- [69] A. Aubry, A. De Maio, Y. Huang, M. Piezzo, and A. Farina, "A New Radar Waveform Design Algorithm with Improved Feasibility for Spectral Coexistence," *IEEE Trans. Aerosp. Electron. Syst.*, vol. 51, no. 2, pp. 1029–1038, April 2015.
- [70] M. Skolnik, *Radar Handbook*, McGraw-Hill, New York, 1990.
- [71] F. Gini, A. De Maio, and L. Pattern, *Waveform Design and Diversity for Advanced Radar Systems*, The Institution of Engineering and Technology, 2012.
- [72] L. Guo, H. Deng, B. Himed, T. Ma, and Z. Geng, "Waveform Optimization for Transmit Beamforming with MIMO Radar Antenna Arrays," *IEEE Trans. Antennas Propagat.*, vol. 63, no. 2, pp. 543–552, February 2015.
- [73] Y. Wang, X. Wang, H. Liu, and Z. Luo, "On the Design of Constant Modulus Probing Signals for MIMO Radar," *IEEE Trans. Signal Processing*, vol. 60, no. 8, pp. 4432–4438, August 2012.
- [74] H. Zang, H. Liu, S. Zhou, and X. Wang, "MIMO Radar Waveform Design Involving Receiving Beamforming," in *International Radar Conference*, October 2014, pp. 1–4.
- [75] S. Sen, "Constant-Envelope Waveform Design for Optimal Target-Detection and Autocorrelation Performances," in *IEEE International Conference on Acoustic, Speech, Signal Processing (ICASSP)*, May 2013, pp. 3851–3855.

- [76] S. Ahmed and M. Alouini, "MIMO Radar Transmit Beampattern Design without Synthesising the Covariance Matrix," *IEEE Trans. Signal Processing*, vol. 62, no. 9, pp. 2278–2289, May 2014.
- [77] X. Zhang, Z. He, L. Rayman-Bacchus, and J. Yan, "MIMO Radar Transmit Beampattern Matching Design," *IEEE Trans. Signal Processing*, vol. 63, no. 8, pp. 2049–2056, April 2015.
- [78] C. Pan, J. Benesty, and J. Chen, "Design of Directivity Patterns with a Unique Null of Maximum Multiplicity," *IEEE/ACM Transactions on Audio, Speech, and Language Processing*, vol. 24, no. 2, pp. 226–235, February 2016.
- [79] Z. Chen, H. Li, G. Cui, and M. Rangaswamy, "Adaptive Transmit and Receive Beamforming for Interference Mitigation," *IEEE Signal Processing Lett.*, vol. 21, no. 2, pp. 235–239, February 2014.
- [80] P. Stoica, J. Li, X. Zhu, and J. R. Guerci, "On Using A-Priori Knowledge in Space-Time Adaptive Processing," *IEEE Trans. Signal Processing*, vol. 56, no. 6, pp. 2598–2602, June 2008.
- [81] G. Hua and S. S. Abeysekera, "MIMO Radar Transmit Beampattern Design with Ripple and Transition Band Control," *IEEE Trans. Signal Processing*, vol. 61, no. 11, pp. 2963–2974, June 2013.
- [82] Y. Xu, X. Zhao, and Y. Liang, "Robust Power Control and Beamforming in Cognitive Radio Networks: A Survey," *IEEE Communications Surveys and Tutorials*, vol. 17, no. 4, pp. 1834–1857, Fourthquarter 2015.
- [83] H. He, P. Stoica, and J. Li, "Wideband MIMO Systems: Signal Design for Transmit Beampattern Synthesis," *IEEE Trans. Signal Processing*, vol. 59, no. 2, pp. 618–628, February 2011.
- [84] O. Aldayel, V. Monga, and M. Rangaswamy, "Tractable Transmit MIMO Beampattern Design under a Constant Modulus Constraint," *IEEE Trans. Signal Processing*, vol. 35, no. 2, pp. 237–246, 2017.
- [85] W. Roberts, J. Li, P. Stoica, and X. Zhu, "MIMO Radar Receiver Design," in *IEEE Radar Conference*, May 2008, pp. 1–6.
- [86] H. Deng and B. Himed, "Interference Mitigation Processing for Spectrum-Sharing Between Radar and Wireless Communications Systems," *IEEE Trans. Aerosp. Electron. Syst.*, vol. 49, no. 3, pp. 1911–1919, July 2013.
- [87] W. Rowe, P. Stoica, and J. Li, "Spectrally Constrained Waveform Design," *IEEE Signal Processing Mag.*, vol. 31, no. 3, pp. 157–162, May 2014.
- [88] L. Patton and B. D. Rigling, "Modulus Constraints in Adaptive Radar Waveform Design," in *IEEE Radar Conference*, May 2008, pp. 1–6.
- [89] L. K. Patton, *On the Satisfaction of Modulus and Ambiguity Function Constraints in Radar Waveform Optimization for Detection*, Ph.D. thesis, Wright State University, June 2009.
- [90] B. Friedlander, "Waveform Design for MIMO Radars," *IEEE Trans. Aerosp. Electron. Syst.*, vol. 43, no. 3, pp. 1227–1238, July 2007.
- [91] A. Aubry, V. Carotenuto, and A. De Maio, "Radar Waveform Design with Multiple Spectral Compatibility Constraints," in *IEEE Radar Conference*, May 2016, pp. 1–6.
- [92] G. Cui, H. Li, and M. Rangaswamy, "MIMO Radar Waveform Design with Constant Modulus and Similarity Constraints," *IEEE Trans. Signal Processing*, vol. 62, no. 2, pp. 343–353, January 2014.
- [93] Z. Luo, W. Ma, A. So, Y. Ye, and S. Zhang, "Semidefinite Relaxation of Quadratic Optimization Problems," *IEEE Signal Processing Mag.*, vol. 27, no. 3, pp. 20–34, 2010.
- [94] P. Stoica, H. He, and J. Li, "On Designing Sequences with Impulse-Like Periodic Correlation," *IEEE Signal Processing Lett.*, vol. 16, no. 8, pp. 703–706, August 2009.
- [95] S. M. Sussman, "Least-Square Synthesis of Radar Ambiguity Functions," *IRE Transactions on Information Theory*, vol. 8, no. 3, pp. 246–254, April 1962.
- [96] R. W. Gerchberg and W. O. Saxton, "A Practical Algorithm for the Determination of Phase from Image and Diffraction Plane Pictures," *Optik*, vol. 35, no. 2, pp. 237–246, 1972.
- [97] O. Aldayel, B. Kang, V. Monga, and M. Rangaswamy, "Technical report: Spatio-spectral radar beampattern design for co-existence with wireless communication systems," Tech. Rep., 2017, Can be found at website : <http://www.personal.psu.edu/osa105/BICTechReport.pdf>.
- [98] S. Boyd and L. Vandenberghe, *Convex Optimization*, Cambridge University Press, 2nd edition, 2004.
- [99] N. J. Higham and S. H. Cheng, "Modifying the Inertia of Matrices Arising in Optimization," *Linear Algebra and its Applications*, vol. 275–276, pp. 261–279, 1998.
- [100] R. A. Horn and C. R. Johnson, *Matrix Analysis*, Cambridge University Press, 2nd edition, 2012.
- [101] V. V. Williams, "Multiplying Matrices Faster than Coppersmith-Winograd," in *Proceedings of the forty-fourth annual ACM symposium on Theory of computing*, May 2012, pp. 887–898.
- [102] H. L. Royden and P. Fitzpatrick, *Real Analysis*, Prentice Hall, 4th edition, 2010.
- [103] C. Chen and P. P. Vaidyanathan, "MIMO Radar Waveform Optimization with Prior Information of the Extended Target and Clutter," *IEEE Trans. Signal Processing*, vol. 57, no. 9, pp. 3533–3544, September 2009.